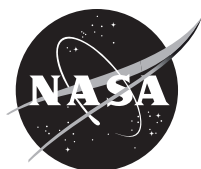


NASA/TM—2019-219979



TURBOMAT: A Probabilistic Turbomachinery Aeroelastic Analysis Tool

Pappu L.N. Murthy
Glenn Research Center, Cleveland, Ohio

T.S.R. Reddy
University of Toledo, Toledo, Ohio

George L. Stefko
Glenn Research Center, Cleveland, Ohio

NASA STI Program . . . in Profile

Since its founding, NASA has been dedicated to the advancement of aeronautics and space science. The NASA Scientific and Technical Information (STI) Program plays a key part in helping NASA maintain this important role.

The NASA STI Program operates under the auspices of the Agency Chief Information Officer. It collects, organizes, provides for archiving, and disseminates NASA's STI. The NASA STI Program provides access to the NASA Technical Report Server—Registered (NTRS Reg) and NASA Technical Report Server—Public (NTRS) thus providing one of the largest collections of aeronautical and space science STI in the world. Results are published in both non-NASA channels and by NASA in the NASA STI Report Series, which includes the following report types:

- TECHNICAL PUBLICATION. Reports of completed research or a major significant phase of research that present the results of NASA programs and include extensive data or theoretical analysis. Includes compilations of significant scientific and technical data and information deemed to be of continuing reference value. NASA counter-part of peer-reviewed formal professional papers, but has less stringent limitations on manuscript length and extent of graphic presentations.
- TECHNICAL MEMORANDUM. Scientific and technical findings that are preliminary or of specialized interest, e.g., “quick-release” reports, working papers, and bibliographies that contain minimal annotation. Does not contain extensive analysis.
- CONTRACTOR REPORT. Scientific and technical findings by NASA-sponsored contractors and grantees.
- CONFERENCE PUBLICATION. Collected papers from scientific and technical conferences, symposia, seminars, or other meetings sponsored or co-sponsored by NASA.
- SPECIAL PUBLICATION. Scientific, technical, or historical information from NASA programs, projects, and missions, often concerned with subjects having substantial public interest.
- TECHNICAL TRANSLATION. English-language translations of foreign scientific and technical material pertinent to NASA's mission.

For more information about the NASA STI program, see the following:

- Access the NASA STI program home page at <http://www.sti.nasa.gov>
- E-mail your question to help@sti.nasa.gov
- Fax your question to the NASA STI Information Desk at 757-864-6500
- Telephone the NASA STI Information Desk at 757-864-9658
- Write to:
NASA STI Program
Mail Stop 148
NASA Langley Research Center
Hampton, VA 23681-2199

NASA/TM—2019-219979



TURBOMAT: A Probabilistic Turbomachinery Aeroelastic Analysis Tool

Pappu L.N. Murthy
Glenn Research Center, Cleveland, Ohio

T.S.R. Reddy
University of Toledo, Toledo, Ohio

George L. Stefko
Glenn Research Center, Cleveland, Ohio

National Aeronautics and
Space Administration

Glenn Research Center
Cleveland, Ohio 44135

January 2019

Acknowledgments

The authors gratefully acknowledge the support of this work provided by the Advanced Air Transport Technology Project (Dr. James Heidmann, project manager, and Mr. Christopher Hughes, subproject manager).

This work was sponsored by the Advanced Air Vehicle Program
at the NASA Glenn Research Center

Trade names and trademarks are used in this report for identification
only. Their usage does not constitute an official endorsement,
either expressed or implied, by the National Aeronautics and
Space Administration.

Level of Review: This material has been technically reviewed by technical management.

Available from

NASA STI Program
Mail Stop 148
NASA Langley Research Center
Hampton, VA 23681-2199

National Technical Information Service
5285 Port Royal Road
Springfield, VA 22161
703-605-6000

This report is available in electronic form at <http://www.sti.nasa.gov/> and <http://ntrs.nasa.gov/>

TURBOMAT: A Probabilistic Turbomachinery Aeroelastic Analysis Tool

Pappu L.N. Murthy
National Aeronautics and Space Administration
Glenn Research Center
Cleveland, Ohio 44135

T.S.R. Reddy*
University of Toledo
Toledo, Ohio 43606

George L. Stefko
National Aeronautics and Space Administration
Glenn Research Center
Cleveland, Ohio 44135

Summary

An integration of aeroelastic analysis procedures with probabilistic analysis methods enables the design of safe reliable engines with quantified reliability. Toward this goal, a graphical user interface (GUI-) based tool that integrates the codes Aeroelastic STability and Response Of Propulsion systems (ASTROP2) two-dimensional analysis and Numerical Evaluation of Stochastic Structures Under Stress (NESSUS) was developed. The tool, entitled “TURBOMachinery Aeroelastic Analysis Tool (TURBOMAT),” was developed utilizing the MATLAB® GUIDE (GUI development environment) (The MathWorks, Inc.) toolbox. TURBOMAT provides a user-friendly computational environment for a rapid assessment of turbomachinery blade flutter characteristics subjected to uncertain loading conditions with variability in material and aerodynamic properties. The tool is seen as an education tool for new students and young engineers starting their careers in structural aeroelasticity who want to learn and understand aeroelastic aspects of turbomachinery components, fans, compressors, and turbines, including uncertainties in loading and material properties.

A typical fan blade configuration geometry was chosen to demonstrate the tool. The results are presented in the form of probabilistic density function (PDF), the cumulative distribution function (CDF), and sensitivity factors. Both first-order fast probability integration (FPI) and the Monte Carlo (MC) techniques are used in the analysis and compared. The tool enabled the quantification of blade flutter reliability as well as the ranking of uncertain variables and their importance to blade flutter response.

1.0 Introduction

Two aeroelastic issues, high cycle fatigue (HCF) due to forced response and catastrophic failure due to flutter, are the drivers of component failures in modern military and civilian gas turbine engines. Accurate computation of these drivers requires an aeroelastic analysis that includes the interaction of unsteady aerodynamics and structural dynamics. A number of aeroelastic analysis codes have been developed for turbomachinery analysis by various Federal agencies, industry, and academia. However, these analysis codes are presently used in a design loop with uncertainties accounted for by using safety

*Resident Research Associate at NASA Glenn Research Center.

factors. This approach yields overly conservative designs, thereby reducing the potential of designing higher efficiency engines. Furthermore, these methods cannot explicitly quantify the reliability of operations.

The Air Force High Cycle Fatigue Group identified uncertainties that had led to many HCF problems. These include uncertainty in anticipating the amplitude of the excitation, identifying the vibration mode and frequency, missing a low order mode, material defects and damage due to manufacturing, and boundary attachments of blades to disks and so on. It is important to account for the uncertainties in order to better estimate the blade stability and life characteristics. A probabilistic analysis cannot only account for uncertainties in the properties of the structure, but it can also provide the probability of occurrence of a failure over the designed life, assisting the designer in making educated choices during design.

An integration of the deterministic aeroelastic analysis procedures with probabilistic analysis methods offers the potential to reduce aeroelastic problems and will provide a quantum leap toward designing safe, reliable engines. Probabilistic analysis will allow for more reliable and efficient engines with lower fuel consumption and reduction in exhaust gas pollutants such as CO₂, NO_x, and hydrocarbons.

Probabilistic applications in the aeroelasticity research area until 2004 have been reviewed in Reference 1. Current research of applications of probabilistic aeroelasticity was presented in References 2 to 11. However, all the applications were for fixed-wing geometry. A simple aeroelastic model was combined with probabilistic analysis for the first time for turbomachinery applications in 2004 (Ref. 12). A mass-spring structural model was used to model the structural dynamic behavior.

The objective of this paper is to improve the structural model in the probabilistic aeroelastic analysis presented in Reference 12. A three-dimensional (3D) structural model will be used in the present analysis, which will allow for probabilistically varying the structural primitive variables. The 3D structural model will be combined with a two-dimensional (2D) unsteady aerodynamic model using strip theory (Ref. 13). The approach taken is to combine the aeroelastic analysis of Aeroelastic STability and Response Of Propulsion systems (ASTROP2) (Refs. 13 and 14) with the fast probability integration (FPI) techniques available in Numerical Evaluation of Stochastic Structures Under Stress (NESSUS) (Refs. 15 and 16). In addition, NESSUS provides the structural dynamic analysis of the blades. The role of ASTROP2 is to provide the functional relationships that tie the structural and aerodynamic parameters (the primitive variables) to the forced response amplitudes and stability eigenvalues (the response properties). The role of FPI is to perform probabilistic analyses by utilizing the response properties generated by ASTROP2. The results are a cumulative distribution function (CDF) for the response properties. CDF is the relationship defined by the value of a response property with respect to its cumulative probability of occurrence. The probabilistic sensitivities of the response variables to uncertainty in primitive variables are obtained as a byproduct of the FPI technique. The results are presented for a fan blade geometry.

Also in the current effort, in addition to developing the formulation and theory for probabilistic aeroelastic analysis methods, a MATLAB[®]-based tool, TURBOMachinery Aeroelastic Analysis Tool (TURBOMAT), was developed by combining ASTROP2 and NESSUS in a seamless manner by using MATLAB[®] programming language (Ref. 17). The emphasis of the current effort is to provide a graphical user interface (GUI-) based platform for the user to expedite the previously mentioned tasks so that rapid assessment of turbomachinery blade performance, aeroelastic stability, and influence of uncertainties is made possible. Further, the code is aimed at minimizing the user's manual intervention, such as running two different codes in a sequential manner, passing the inputs and outputs appropriately between the codes, culling the outputs of the respective codes in order to analyze the results, and use of a spreadsheet tool or some other means to visualize graphically the results. With the aid of the current tool, all these operations can be done by simply navigating within the GUI. The results are displayed in graphical form. Often, it is not uncommon for a user to spend several hours to do the above, whereas the current tool can

do all of the above operations in a matter of seconds. In addition, costly errors due to manual operations are easily avoided.

The report is organized as follows. First the formulation of the aeroelastic governing equations is presented. Then the formulation for probabilistic analysis is given, including the procedure for FPI analysis followed by the steps involved in the analysis. Next, the details and usage of the GUI tool developed using MATLAB[®] programming language are provided. Aeroelastic analysis results and deterministic and probabilistic analysis results for flutter are then presented. Both FPI and Monte Carlo (MC) analysis procedures are illustrated and the results are compared.

The report ends with two illustrative examples. The first one pertains to a deterministic Aeroelastic assessment of the SR3C–X2 propfan for which experimental data is available. This example is used for the purpose of validation of the methodology presented here. The second example illustrates probabilistic risk assessment for a typical fan blade flutter.

2.0 Formulation

As previously mentioned, the present work adopts an integrated modular approach, which is a synergistic combination of three research disciplines supported by NASA Glenn Research Center. The first methodology is concerned with ASTROP2, an aeroelastic stability and response analysis code for turbomachines. The second one involves structural analysis with NESSUS. The third one consists of a NESSUS/FPI technique that takes into account the uncertainties in structural and aerodynamic parameters of the turbomachinery components, and provides a probabilistic assessment of the aeroelastic system. A synergistic combination of these three methodologies leads to the development of a GUI-based user-friendly tool, TURBOMAT, that uses MATLAB[®] programming language for easy operation and visualization of results. A description of the aeroelastic simulation and probabilistic simulation is given in the following section.

2.1 Aeroelastic Simulation

In general, the components of a fan compressor or turbine have complex geometries. A finite element model will accurately predict the structural dynamic behavior of the blades. To accomplish the stated objectives of the paper, it is necessary to use a model that simplifies the analysis, yet maintains the basic structural and aerodynamic characteristics. The ASTROP2 code (Refs. 13 and 14) uses the data from the finite element structural analysis and combines 2D aerodynamic models to calculate flutter eigenvalues and forced response magnitudes of turbomachine components: fan, compressor, or turbine. A brief description of the models and governing equations of motion is given in the following subsections.

2.1.1 Aerodynamic Model

The unsteady aerodynamic loads are calculated using Smith's theory in subsonic flow (Ref. 18) and Adamczyk and Goldstein's theory for supersonic flow with a subsonic leading edge (Ref. 19). In these 2D theories, the effect of airfoil thickness, camber, and steady-state angle of attack are neglected, and the flow is assumed to be isentropic and irrotational. The effect of wakes shed from upstream periodic obstructions is included. The wakes are limited to sinusoidal distortions represented by vorticity perturbations so that they are convected downstream at the flow velocity.

2.1.2 Structural Model

The structural dynamic solution is obtained from a finite element model solution using NESSUS structural analysis code (Ref. 16). The code is based on a mixed-iterative finite element formulation

derived from a three-field variational principle, with the displacements, strains, and stresses obtained directly at the nodes of the finite element mesh. It provides a choice of algorithms for the solution of static and dynamic problems, both linear and nonlinear. The possible type of structural analyses include static analysis, dynamic eigenvalue analysis, transient dynamics, buckling eigenvalue analysis, and harmonic and random excitation analysis. There are about 10 element types available for analysis (for more information, see Ref. 16). For aeroelastic computations, the dynamic eigenvalue analysis is utilized that provides generalized mode shapes, generalized frequencies, and generalized masses of the 3D blade. The 3D dynamic eigenvalue solution is integrated with the 2D unsteady aerodynamic solutions by using the method of strips. In this method, the 3D blade is divided into a number of strips at which the 2D unsteady aerodynamic forces are calculated and summed over the entire length of the blade.

3.0 Aeroelastic Model

A normal modes approach is used for the aeroelastic analysis. The equations of motion for the k^{th} blade of the cascade for P normal modes can be written as

$$[M]_{P \times P}^k \{\ddot{\eta}\}_{P \times 1}^k + [K]_{P \times P}^k \{\eta\}_{P \times 1}^k = \{\mathbf{f}^{\eta}_a\}_{P \times 1}^k + \{\mathbf{f}_a\}_{P \times 1}^k \quad (1)$$

where $[M]^k$ and $[K]^k$ are generalized mass and stiffness matrices for the k^{th} blade, η is the generalized displacement vector, and $\{\mathbf{f}^{\eta}_a\}$ is the motion-dependent aerodynamic load vector, $\{\mathbf{f}_a\}$ is the motion-independent aerodynamic load vector, and $\{\ddot{\eta}\}^k$ is the generalized coordinates for the k^{th} blade. The motion-dependent forces cause flutter, and motion-independent forces cause forced response (forced vibration). The elements of the matrices $[M]^k$ and $[K]^k$ are given by a free vibration analysis from NESSUS. The expressions for $\{\mathbf{f}^{\eta}_a\}^k$ and $\{\mathbf{f}_a\}^k$ using strip theory are given in Equations (3), (4), and (5).

In ASTROP2 the blades are divided into strips where the aerodynamic forces are calculated, see Figure 1(a). Each strip has two degrees of freedom, a plunging displacement motion perpendicular to the chord, h , and a pitching (torsion) displacement rotation about the leading edge of the strip, α (Figure 1(b)). Using the normal modal values obtained from a free vibration analysis, the equivalent plunging displacement perpendicular to the chord, h , and pitching displacement about the leading edge of a strip, α , for the m^{th} strip of the k^{th} blade are given as summation of normal modes as

$$\{u_m\}^k = \begin{Bmatrix} h_m \\ \alpha_m \end{Bmatrix}_{2 \times 1} = \begin{bmatrix} h_{m1} h_{m2} \cdots h_{mP} \\ \alpha_{m1} \alpha_{m2} \cdots \alpha_{mP} \end{bmatrix}_{2 \times P} \begin{Bmatrix} \eta_1 \\ \eta_2 \\ \vdots \\ \eta_P \end{Bmatrix}_{P \times 1} \quad (2a)$$

where P is the number of normal modes, or

$$\{u_m\}^k = [\phi_m]^k \{\eta\}^k \quad (2b)$$

where $[\phi_m]$ is the modal matrix for the m^{th} strip.

It should be noted that when using ASTROP2, only the location of the strips has to be input to the code. ASTROP2 calculates the h and α values at these strips, and uses them in the analysis; that is, the user need not input the h and α values at each strip for each mode.

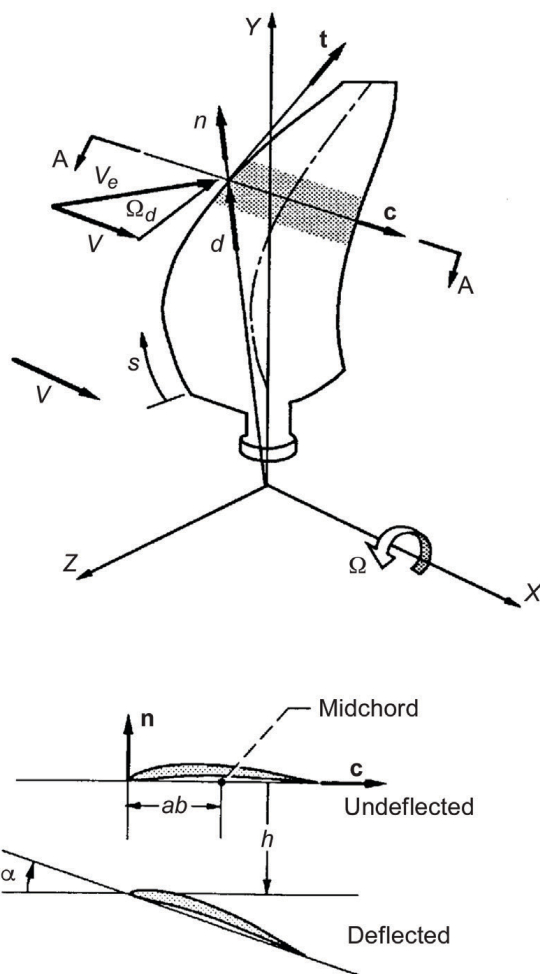


Figure 1.—Typical section blade (A-A) model with two degrees of freedom (Ref. 13), where ab is the distance from leading edge to elastic center, c is chord vector, d is midpoint distance, h is plunging distance perpendicular to chord, n is normal vector, s is arc length measured along leading edge, t is tangent vector, V is axial velocity, V_e is effective velocity, α is pitching displacement rotation about leading edge of strip, and Ω is rotational speed.

The motion-dependent aerodynamic forces $\{\mathbf{f}_a^\eta\}^k$ are given by

$$\{\mathbf{f}_a^\eta\}^k = \omega^2 [\phi^k]^T_{P \times 2M} \{\mathbf{F}\}^k_{2M \times P} \quad (3)$$

where ω is the assumed frequency at which the aerodynamic forces are calculated, $[\phi^k]$ is the modal matrix for the k^{th} blade, and $\{\mathbf{F}\}^k$, the aerodynamic force vector for the k^{th} blade, is given as

$$\{\mathbf{F}\}_{2M \times P}^k = \sum_{n=1}^{NB} [\Psi]_{2M \times 2M}^{kn} [\Phi]_{2M \times P}^n \{\boldsymbol{\eta}\}_{P \times 1}^n \quad (4)$$

where NB is the number of blades, n is the number of random variables, and M is the total number of strips used in the analysis. The motion-independent aerodynamic forces, $\{\mathbf{f}_a\}^k$, are given by

$$\{\mathbf{f}_a\}^k = \omega^2 \{G\}_{P \times 1}^k \quad (5)$$

For the present analysis, the aerodynamic force coefficients in Equations (4) and (5) are obtained using the linear unsteady aerodynamic models of References 18 and 19. Where $[\phi_m]$ represents the assembled modal matrix for the m^{th} strip, ω is the assumed frequency for which aerodynamic forces are calculated, $[\Psi]$ and $\{G\}$ are the assembled motion-dependent and motion-independent load matrices, respectively. The elements of these matrices are provided in Reference 20.

With the aid of Equations (3) and (5), Equation (1) can be written as

$$[M]^k \{\ddot{\boldsymbol{\eta}}\}^k + [K]^k \{\boldsymbol{\eta}\}^k = \omega^2 \sum_{n=1}^{NB} [A]_{P \times P}^{kn} \{\boldsymbol{\eta}\}^n + \omega^2 \{G\}^k \quad (6)$$

where

$$[A]_{P \times P}^{kn} = [\phi^k]_{P \times 2M}^T [\Psi]_{2M \times 2M}^{kn} [\phi^n]_{2M \times P} \quad (7)$$

where T is transpose and $[A]$ is the motion-dependent aerodynamic force matrix on the k^{th} blade from all blades. It should be noted that Equation (7) permits the use of mode shapes that differ from blade to blade.

By writing Equation (7) for all blades, the equations of motion for the cascade can be written as

$$[M_g] \{\ddot{\mathbf{X}}\} + [K_g] \{\mathbf{X}\} = \omega^2 [A] \{\mathbf{X}\} + \omega^2 \{G\} \quad (8)$$

where $[K_g]$ and $[M_g]$ are the assembled global stiffness and assembled global mass matrices of all blades, respectively, $\{\ddot{\mathbf{X}}\}$ is the time derivative of the vector of the generalized coordinates, and $\{\mathbf{X}\}$ is the vector of the generalized components of all the blades. Assuming the solution for Equation (8) is of the form

$$\{\mathbf{X}\} = \{\bar{\mathbf{X}}\} e^{i\omega t} \quad (9)$$

where e is the exponential value, t is the time, and $\{\bar{\mathbf{X}}\}$ is the vector of the amplitude of the generalized coordinates, and dividing both sides by an assumed frequency, ω_0^2 , and rearranging, Equation (8) can be written as

$$[[P] - \gamma [Q]] \{\bar{\mathbf{X}}\} = \gamma \{G\} \quad (10)$$

where

$$[P] = \frac{1}{\omega_0^2} [K_g] \quad (11a)$$

$$[Q] = [M_g] + [A] \quad (11b)$$

$$\gamma = \left[\frac{\omega^2}{\omega_0^2} \right] \quad (11c)$$

For a stability calculation (flutter), the motion-independent forces $\{G\}$ are set to zero and the eigenvalue problem is obtained in the standard form of

$$[[P] - \gamma[Q]]\{\bar{X}\} = \{0\} \quad (12)$$

The solution of the previous eigenvalue problem, Equation (12), results in a total of $NB \times P$ complex eigenvalues of the form

$$i \left(\frac{\omega}{\omega_0} \right) = i\sqrt{\gamma} = \mu + i\nu \quad (13)$$

The real part of the eigenvalue, μ , represents the damping ratio, the imaginary part, ν , represents the damped frequency, and i is the imaginary value; flutter occurs if $\mu \geq 0$ for any of the eigenvalues.

The aeroelastic response of the blades induced by wakes is calculated from Equation (10) as

$$\{\bar{X}\} = [[P] - \gamma[Q]]^{-1} \gamma\{G\} \quad (14)$$

3.1 Tuned Cascade

For a tuned cascade in which all the blades have identical structural properties, the interblade phase angle modes are uncoupled. The equation of motion can be solved for each interblade phase angle, given by

$$\sigma_j = 2 * \pi(j / NB); j = 0, 1, 2, \dots, R \dots NB - 1 \quad (15)$$

where j is the counter.

For tuned cascade analysis and the R^{th} interblade phase angle, Equation (6) can be written as

$$[M]^k \{\ddot{\eta}\}^k + [K]^k \{\eta\}^k = \omega^2 [A]^R \{\eta\} + \omega^2 \{G\}^R \quad (16)$$

Since the blades are identical, the same equation is obtained for each blade and superscript k can be dropped.

Equation (16) is solved for NB different values of the interblade phase angle given by Equation (15). It is to be noted here that the size of the matrices for solution is now reduced to $P \times P$ compared to $NBP \times NBP$ for mistuned case. As before, the equations for the stability (flutter) problem are obtained by setting the motion-independent forces to zero. For a given interblade phase angle, the solution of the eigenvalue problem results in P complex eigenvalues of the form given by Equation (13) and flutter

occurs if $\mu \geq 0$ for any of the eigenvalues. The eigenvalue problem is solved for each of the NB permissible values. The critical phase angle is identified as the one that results in the lowest flutter speed.

3.2 Probabilistic Simulation

There are a number of approaches available for obtaining a probabilistic response from a set of independent variables and the expressions describing the response behavior. MC simulation is one such fairly common technique for obtaining the CDFs given the probability distributions of independent variables. In this technique, randomly selected values of the input variables, which are based on their known probabilistic distributions, are used to deterministically compute the value of the response variable. This must usually be repeated hundreds or even thousands of times to build the probabilistic characteristics. In essence, this technique requires a large number of simulations to generate CDFs of output variables. Although, inherently simple, the large number of output sets that must be generated to obtain a reasonably accurate CDF of output variables becomes an obvious disadvantage. Glenn has been involved in developing efficient probabilistic methods for more than a decade. As a result of this research initiative, FPI algorithms were developed (Ref. 15) to solve a large class of engineering problems.

Let $Z(X)$ represents a function of n random variables X_1 through X_n as shown below:

$$Z(X) = Z(X_1, X_2, \dots, X_n) \quad (17)$$

The aim is to compute the probability that Z will have a value less than or equal to a given magnitude Z_0 . To achieve this goal, the performance function, which describes how the mechanics of the system behave, can be cast as a limit state function $g(X)$, which can be described as

$$g(X) = Z(X) - Z_0 \quad (18)$$

Traditionally, the limit state function g has been defined in such a way that $g = 0$ represents a boundary where $g < 0$ represents failed region and $g > 0$ represents safe region. Here, the objective would be to compute $P[g(X) \leq 0]$. Generally speaking, Z_0 describes a limit indicating failure, $g(X)$ is called a failure function or in a classical sense, the probability of the stress exceeding the strength.

Given the probability density function $f_x(x)$ of the limit state function $g(X)$, the limit state probability $P[g \leq 0]$ can be formulated as

$$P_f = P[g(X) \leq 0] = \int_{\Theta} \dots \int f_x(x) dx \quad (19)$$

where Θ describes the domain of integration and f is the function. This multiple integration is, in general, very difficult to integrate analytically. However, FPI has been found to be an excellent tool to evaluate Equation (19) efficiently and accurately.

3.2.1 Implementation of Probabilistic Procedure by Using Fast Probability Integration (FPI)

A brief schematic of the FPI input and output scheme is shown in Figure 2. It is a probabilistic analysis tool that implements a variety of methods for probabilistic analysis. The procedure for the probabilistic analysis is as follows:

- (1) Identify the independent and uncorrelated design (primitive) variables with uncertainties (i.e., identify the risk elements).

- (2) Quantify the uncertainties of these design variables with probability distributions based on expert opinion, historical data, or benchmark and prototype testing and so on.
- (3) It is required that there is a response function (sometimes called a performance function) that defines the relationship between the response and the independent variables. For the present study, the solution from the ASTROP2 code defines the response function that relates the structural and aerodynamic design variables to the response. For an aeroelastic analysis, the flutter eigenvalues that indicate aerodynamic damping and forced response amplitude are the response quantities.
- (4) For a given set of values of primitive variables, the ASTROP2 code is used to generate the desired response variables. The whole process is repeated a number of times to generate a table of response variable values that correspond to the perturbed values of the primitive variables. The number of simulations needed depends upon the method used and the number of random variables, but they are far less than what would be required in a standard MC technique.
- (5) The FPI then uses the table of responses obtained in step (4) to compute the CDF, PDF, and the corresponding sensitivities of the response to primitive variables.

Several methods are available in the FPI to compute a probabilistic distribution. In addition to obtaining the CDF and PDF of the response, the FPI provides additional information regarding the sensitivity of the response with respect to the primitive variables. They provide valuable information in controlling the scatter of the response variable. The random primitive variable with the highest sensitivity factor will yield the biggest payoff in controlling the scatter in that particular response variable. Such information is very useful to the test and design engineers for designing or interpreting the measured data.

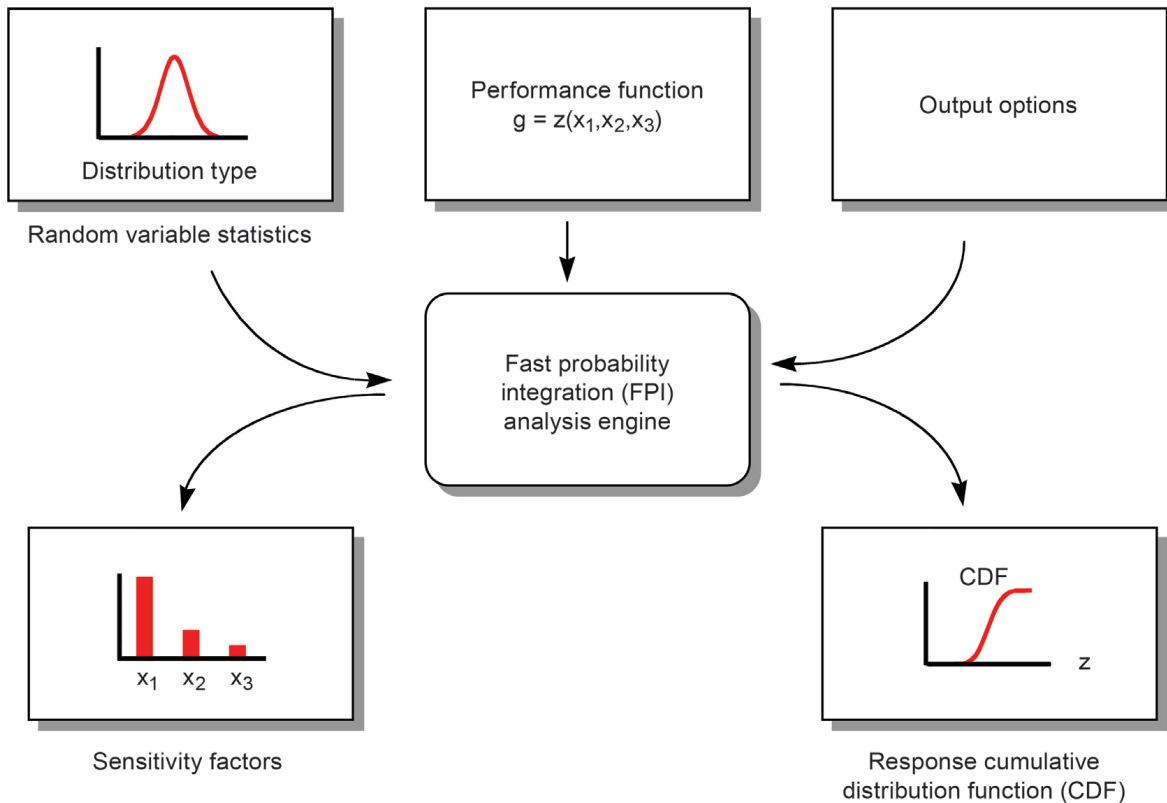


Figure 2.—Fast probability integration input/output process flow.

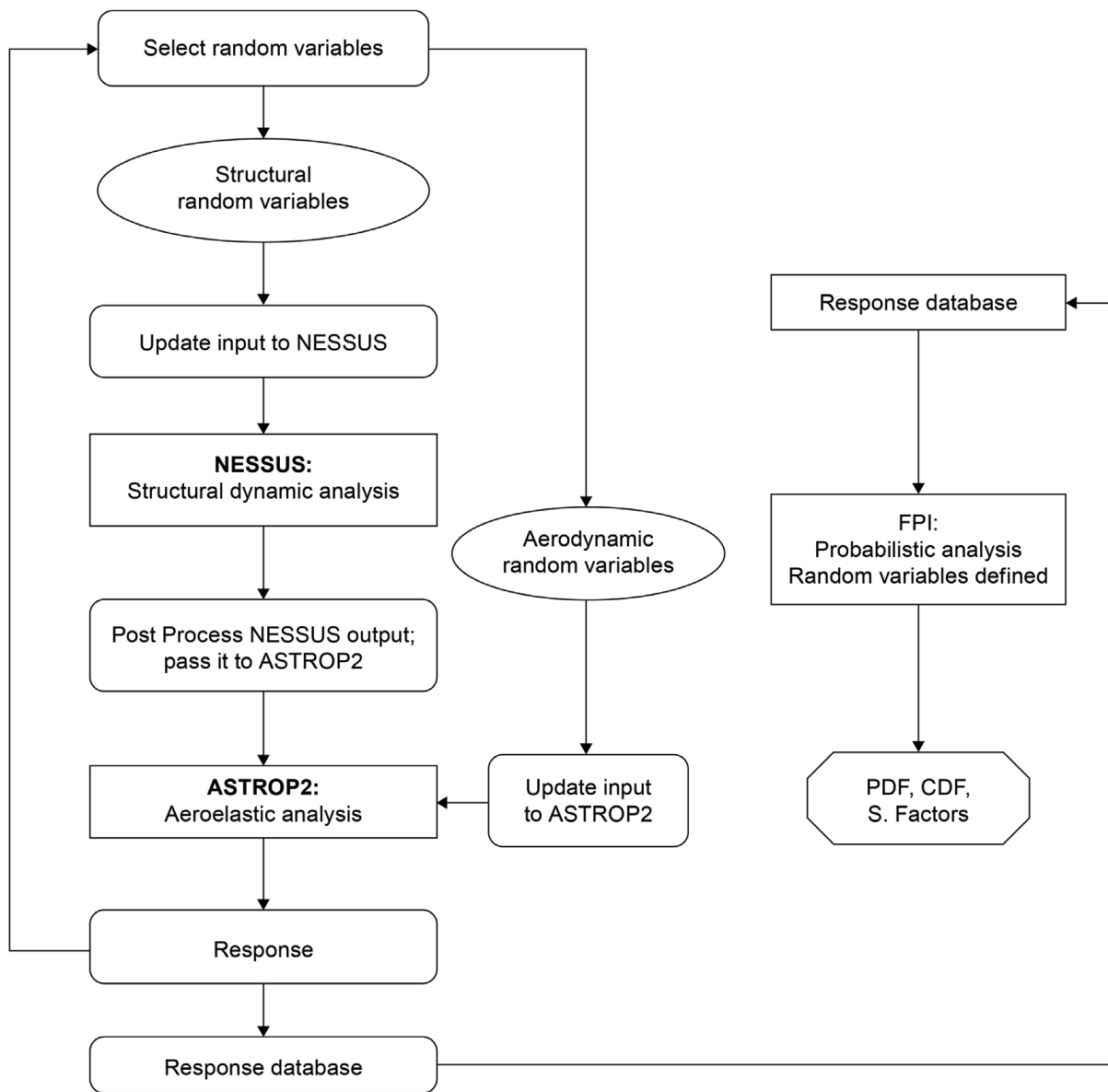


Figure 3.—Probabilistic aeroelastic analysis module setup.

3.3 Program Flow Chart and TURBOMachinery Aeroelastic Analysis Tool (TURBOMAT)

The steps required for the probabilistic aeroelastic analysis are shown in Figure 3. In the first step, the random variables (random.in) are selected. For the structural random variables, the finite element input deck to NESSUS, struc.dat, is updated with new values of the primitive variables using a separate program developed for this purpose. A dynamic structural analysis using NESSUS is done for the free vibration analysis giving an output file containing vibration frequencies, generalized masses, and mode shapes. For the aerodynamic random variables the input deck, astrop2.in, to ASTROP2 is updated with new values of the primitive variables using a separate program developed for this purpose. The aeroelastic analysis is done using ASTROP2 with its own input deck along with the output of NESSUS dynamic

structural analysis done earlier. The output of ASTROP2, aerodynamic damping and frequency are recorded for each random variable to form a database. This database is used to prepare the input deck for FPI and to run FPI for probabilistic analysis that gives the CDF, PDF, and sensitivities.

In TURBOMAT, NESSUS is used to first perform a structural analysis on blades to determine its natural frequencies and mode shapes. These are fed as input to the fluids code in ASTROP2 (Refs. 18 and 19). The results from ASTROP2 are then utilized to form an appropriate input to NESSUS/FPI. NESSUS/FPI performs probabilistic assessment of response to uncertainties in material properties, geometrical variations, and loading uncertainties. Thus, NESSUS is utilized to perform both preprocessing and postprocessing operations in TURBOMAT.

4.0 Results and Discussion

A fan configuration with 24 blades is considered for aeroelastic (flutter and/or stability) analysis and for probabilistic analysis. This configuration consists of a rotor with twisted flat-plate blades enclosed in a cylindrical duct with no tip gap. This configuration was developed in Reference 21 to provide a relatively simple test case for comparison with 2D analyses. It is referred to in literature as “the helical fan configuration.” Note that there is no experimental data available for this configuration.

The parameters for this configuration are such that the midspan location corresponds to a flat-plate cascade with a stagger angle of 45° , unit gap-to-chord ratio, operating in a uniform mean flow at a Mach number, M , of 0.7 parallel to the blades. The radius at the hub is 8.619 cm (3.395 in.) and the radius at the tip is 10.775 cm (4.244 in.) with a hub-to-tip ratio of 0.8. The inlet flow (axial) Mach number is 0.495, and the rotation speed of the fan is 16,962 rpm, giving a relative Mach number of approximately 0.7 at the midspan section.

4.1 Design and Response Variables for the Numeric Example

There are eight design parameters that are considered for the analysis which are described in this section. For probabilistic analysis, any of the design variables can be used as the variables with uncertainty. In the present analysis, all eight parameters are considered for the probabilistic analysis. Flat-plate airfoils are considered for aerodynamic analysis. The unsteady aerodynamic coefficients for the aeroelastic analysis are obtained using the Smith code (Ref. 18) for subsonic flow and from the Adamczyk and Goldstein code (Ref. 19) for supersonic flow with a subsonic leading edge.

The design variables with their notation in parenthesis are given in the following table.

Design variable	Description	Notation
β	Setting angle	BETA
E	Blade material Young's modulus	(YMOD)
ν	Blade material Poisson's ratio	(POIS)
ρ	Mass density of blade material	(MASSD)
t	Blade thickness parameter	(THICKD)
N	Blade rotational speed	(RPM)
P_0	Static aerodynamic pressure	P0
a_∞	Speed of sound	A0

TABLE I.—DESIGN VARIABLES WITH UNCERTAINTIES

Design variable	Deterministic value	Mean	Standard deviation, percent	Distribution
Setting angle, β	44.74	44.74	5	Normal
Young's modulus, E	0.16×10^8	0.16×10^8	5	Normal
Poisson's ratio, ν	0.3	0.3	5	Normal
Mass density, ρ	0.4144×10^{-3}	0.4144×10^{-3}	5	Normal
Thickness, t	1.0	1.0	5	Normal
Rotational speed, N	16,962	16,962	5	Normal
Static pressure, P_0	14.4057	14.4057	5	Normal
Speed of sound, a_∞	1142.25	1142.25	5	Normal

For the design variables, BETA, YMOD, POIS, MASSD, THICKD, and RPM affect the vibration characteristics—frequencies and mode shapes—and BETA, RPM, P0, and A0, along with the free-stream Mach number, affect the unsteady aerodynamic forces. Air density depends on the pressure ratio and temperature, and affects both the Mach number and air mass. The assumed mean values and standard deviations of these variables are given in Table I. These variables are assumed to be independent and have normal distributions.

The response variables are flutter frequency (modes 1 and 2) and flutter damping (modes 1 and 2).

4.2 Validation of Structural Model Frequency Comparison

One of the goals of the current effort is to use inhouse codes. So it was decided to use the NESSUS structural analysis capability that was developed as a part of Glenn sponsorship, and the code is freely available for NASA use. As a first step, the frequencies obtained from ANSYS® in Reference 20 for the same geometry are compared with those predicted by NESSUS to assess the suitability of NESSUS in free vibration analysis and for subsequent aeroelastic analysis. The finite element model has 891 nodes and 800 elements. In NESSUS, the blade is modeled with the four-noded quadrilateral element, Element 75. This is a bilinear, isoparametric, variable-thickness shell element based on the Reissner-Mindlin plate and shell theories. It has three translational displacements and three rotations at each node. Table II shows the first two vibration frequencies predicted by ANSYS® and NESSUS for a nonrotating and rotating blade. NESSUS predictions show excellent agreement with those obtained by ANSYS® for this case. It should also be noted that the software developed is modular and individual analysis modules can be replaced easily by other structural analysis codes if needed.

5.0 TURBOMachinery Aeroelastic Analysis Tool (TURBOMAT) Graphical User Interface (GUI)

Figure 4 shows the GUI layout of TURBOMAT. This tool is developed by using the MATLAB® GUI development environment (GUIDE) toolbox in the Microsoft Windows personal computer environment. The design of the GUI follows context-sensitive windows, tables, and buttons in the sense that depending on the user's choice, only the appropriate windows and buttons are shown, and all the other details are suppressed. This gives the interface a clean and uncluttered look. Furthermore, context-sensitive helpful tips for all the user choices are provided to give appropriate hints pertaining to the inputs by hovering the mouse pointer over the button on box. The next few paragraphs describe step-by-step introduction of the various tables, buttons, and boxes that need to be filled by the user.

TABLE II.—PREDICTED FREQUENCIES IN HERTZ FOR A HELICAL FAN

Mode	ANSYS®	NESSUS ^a	Difference, percent
Nonrotating blade			
1	363.56	362.34	0.3
2	1744.77	1740.12	0.3
Blade rotating at 16,962 rpm			
1	821.59	847.56	0.3
2	1882.30	1899.82	0.4

^aNumerical Evaluation of Stochastic Structures Under Stress.

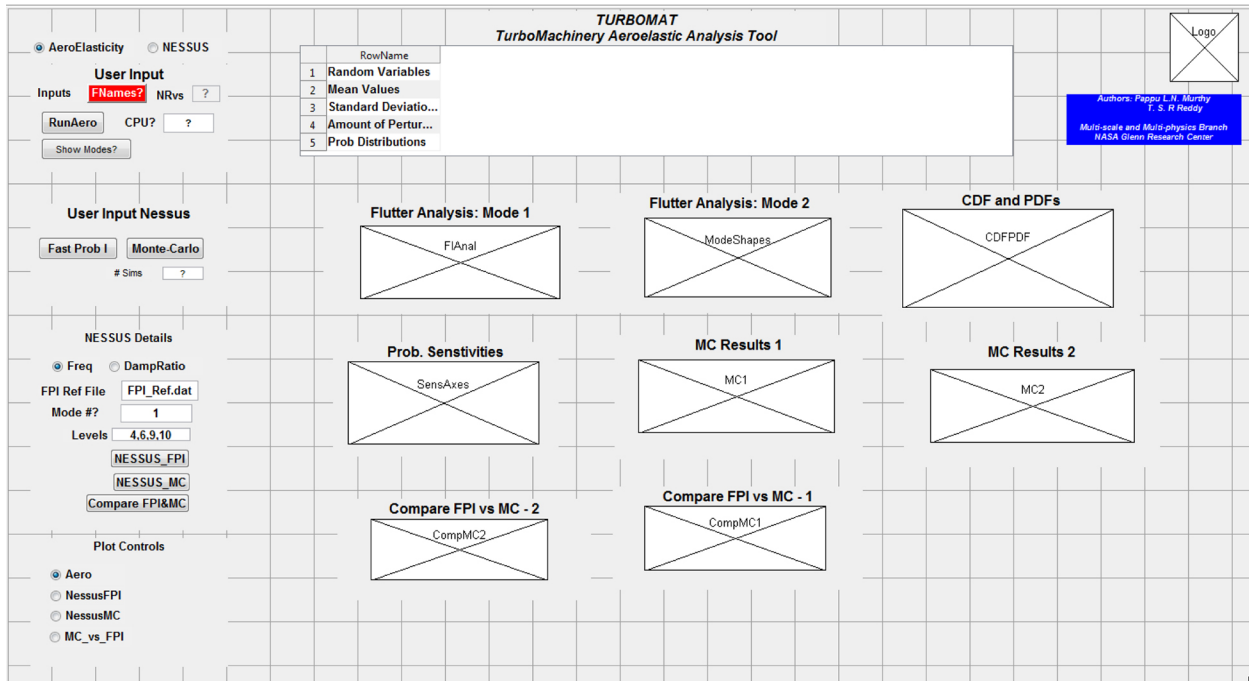


Figure 4.—TURBOMAT graphical user interface, where CDF is cumulative distribution function, CPU is central processing unit, FPI is fast probability integration, MC is Monte Carlo, NEUSS is Numerical Evaluation of Stochastic Structures Under Stress, and PDF is probabilistic density function.

5.1 Aeroelastic Analysis (Deterministic Mode)

When a user starts the program for the first time, two panels appear. The first one has two radio buttons, one for choosing AeroElasticity analysis and the other one for NESSUS analysis. The user must choose one of the two. The AeroElasticity radio button, if chosen, invokes a deterministic run where the aeroelastic analysis determines the flutter response of the blade for the user given variable information. The second radio button if chosen, starts the process for probabilistic aeroelasticity analysis using NESSUS program. The second panel consists of a button, FNames?, and an editable text box, NRvs. The red FNames? button turns green once pushed and after filling in the necessary input file names, astrop2.in, random.in, and struc.dat. The details of astrop2.in, random.in, and struc.dat are given in Appendixes B, C, and D, respectively. The struc.dat file is too big and only portions of the file are provided here for completeness. Figure 5 and Figure 6 show the details pertaining to these two panels. Once the necessary input file names are supplied, the red button changes color to green. Next, the user is

required to fill in the input variable details by first specifying the number of variables involved in the analysis. For these examples, there are eight variables. As soon as the box is filled, a new input table appears on the right, consisting of five rows and eight columns (Figure 7).

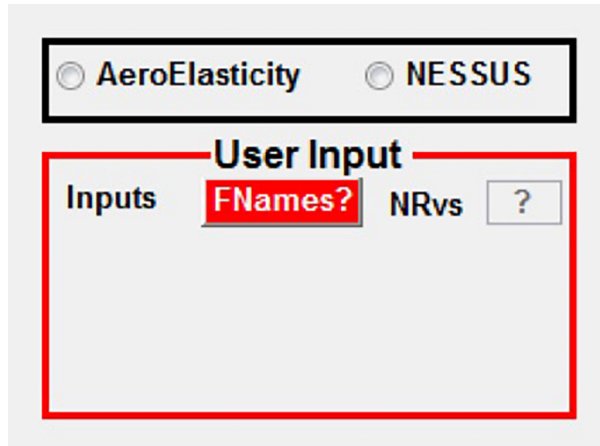


Figure 5.—Starting dialogue where user needs to choose analysis module and supply necessary input file names, number input variables to aeroelastic analysis, and so on.

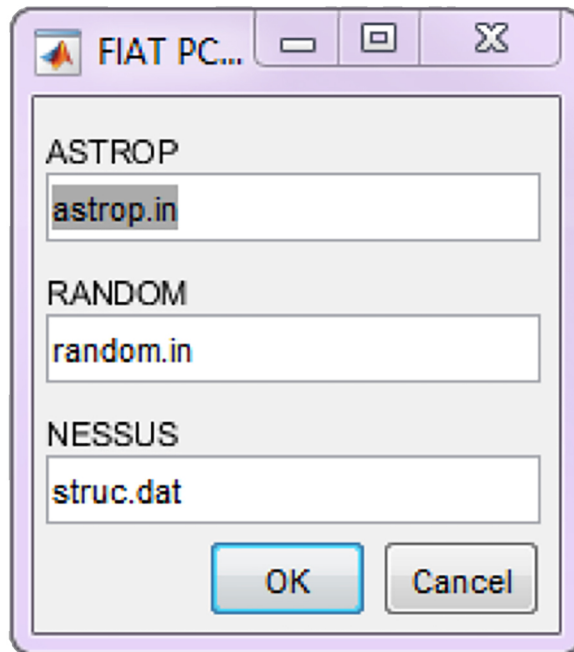


Figure 6.—Dialogue box that appears when FNames? button is pushed. Here, user inputs appropriate file names for ASTROP2 input (astrop2.in), RANDOM (random.in), and Numerical Evaluation of Stochastic Structures Under Stress (NESSUS) input (struc.dat).

TURBOMAT Ver. 3.6
TurboMachinery Aeroelastic Analysis Tool

	RowName	Var1	Var2	Var3	Var4	Var5	Var6	Var7	Var8
1	Random Variables	BETA	E	NU	RHO	t	N	P0	A0
2	Mean Values	44.7400	16000000	0.3000	4.1440e-04	1	16962	14.4057	1.1423e+03
3	Standard Deviatio...	2.2370	800000	0.0150	2.0720e-05	0.0500	848.1000	0.7203	57.1125
4	Amount of Pertur...	1	1	1	1	1	1	1	1
5	Prob Distributions	Normal	Normal	Normal	Normal	Normal	Normal	Normal	Normal

Figure 7.—Details of input variables needed for aeroelastic analysis as well as probabilistic aeroelastic analysis. Values shown in table are default values.

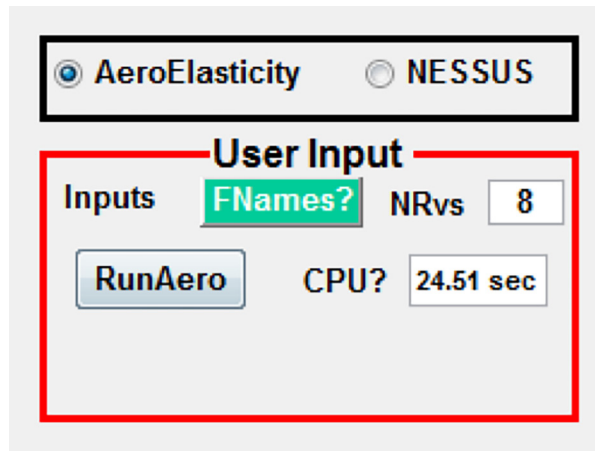


Figure 8.—Running deterministic aeroelastic analysis took 24.51 s.

The first row shows the description of the eight variables. These are β , E , ν , ρ , t , N , P_0 , and a_∞ . The table already has default values filled in. The second row consists of the mean values for the eight variables. The third row consists of standard deviations for each of the variables. These values are used in NESSUS FPI probabilistic analysis and are ignored during the deterministic aeroelastic analysis. The fourth row consists of amount of perturbation to consider for probabilistic analysis. Usually this is equal to one standard deviation from the mean, however, the user may choose a different value. The fifth row is filled in with the name of probabilistic distribution. Currently, only normal distribution is supported. Other distribution types can and will be added in future.

Once the necessary inputs are provided for the choice of aeroelastic analysis, a new button, RunAero, appears. Pushing this button results in performing both structural analysis for modal information and ASTROP2 analysis for the blade's aeroelastic performance. At the end of the analysis, an additional box appears where the CPU time taken for the entire operation is shown. In this particular case, the analysis took 24.51 s, as shown in Figure 8.

Figure 9 shows the root locus plot and damping versus frequency ratio for an assumed flutter frequency of 1,527 Hz for the two modes considered in the analysis. The values are given for all possible 24 phase angles for a 24-bladed rotor. As can be seen from the plots, the damping is negative for both the modes and for all possible phase angles. This implies that for the selected deterministic structural and aerodynamic parameters, the structure is aeroelastically stable, that is, no failure due to flutter.

The critical phase angle, the phase angle for which the damping ratio is minimum, is 45° . In the subsequent probabilistic analysis, the 45° phase angle will be used for the probabilistic assessment of the blade flutter response. It was noted that the critical phase angle did not change for the standard deviations considered for the variables.

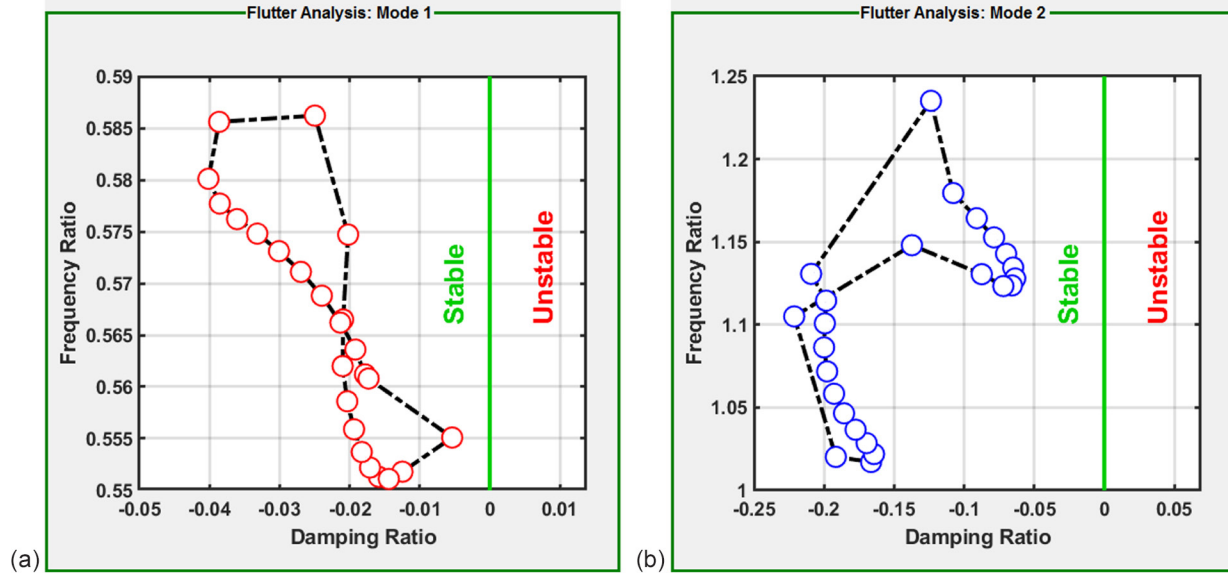


Figure 9.—Results of deterministic aeroelastic analysis for first two modes.

5.2 Probabilistic Analysis (Numerical Evaluation of Stochastic Structures Under Stress (NESSUS))

For the probabilistic analysis mentioned in Section 5.2, the user chooses the radio button NESSUS. Probabilistic analysis has two modes of operation. One is the FPI technique. The second one is the conventional MC technique, which involves running thousands of aeroelastic analyses by choosing a random input configuration for each run picking up the variable instances from their respective probabilistic distributions. The input details required for NESSUS were explained previously and shown in Figure 7. This input is common for both NESSUS/FPI analysis and MC simulations. NESSUS/FPI analysis involves running aeroelastic analysis and collecting the response for $(2 * n + 1)$ cases of input, where n is number of random variables. In this case, $n = 8$, and therefore for NESSUS/FPI, exactly 17 runs are needed. For MC analyses, typically a minimum of 1,000 simulations are recommended. The MC results presented in the document are based on 1,000 simulations.

5.2.1 Numerical Evaluation of Stochastic Structures Under Stress (NESSUS)/Fast Probability Integration (FPI) Analysis

When the user chooses NESSUS as the analysis option, two additional panels appear, as seen in Figure 10(a). The user has the option of choosing either Fast Prob I or Monte-Carlo. Figure 10(b) is the result of choosing the option Fast Prob I. There are 17 total aeroelasticity analyses and the total CPU time taken is 117.26 s, as shown in Figure 10(b). At this stage, all the analyses are complete and the program waits for user choices for depicting the results in graphical form. Several choices are available, as can be seen in panel NESSUS Details. The user has the option of choosing frequency response or damping ratio (flutter) response as indicated by the radio buttons Freq and DampRatio, respectively. For each of these, the user can choose either the first or second natural mode.

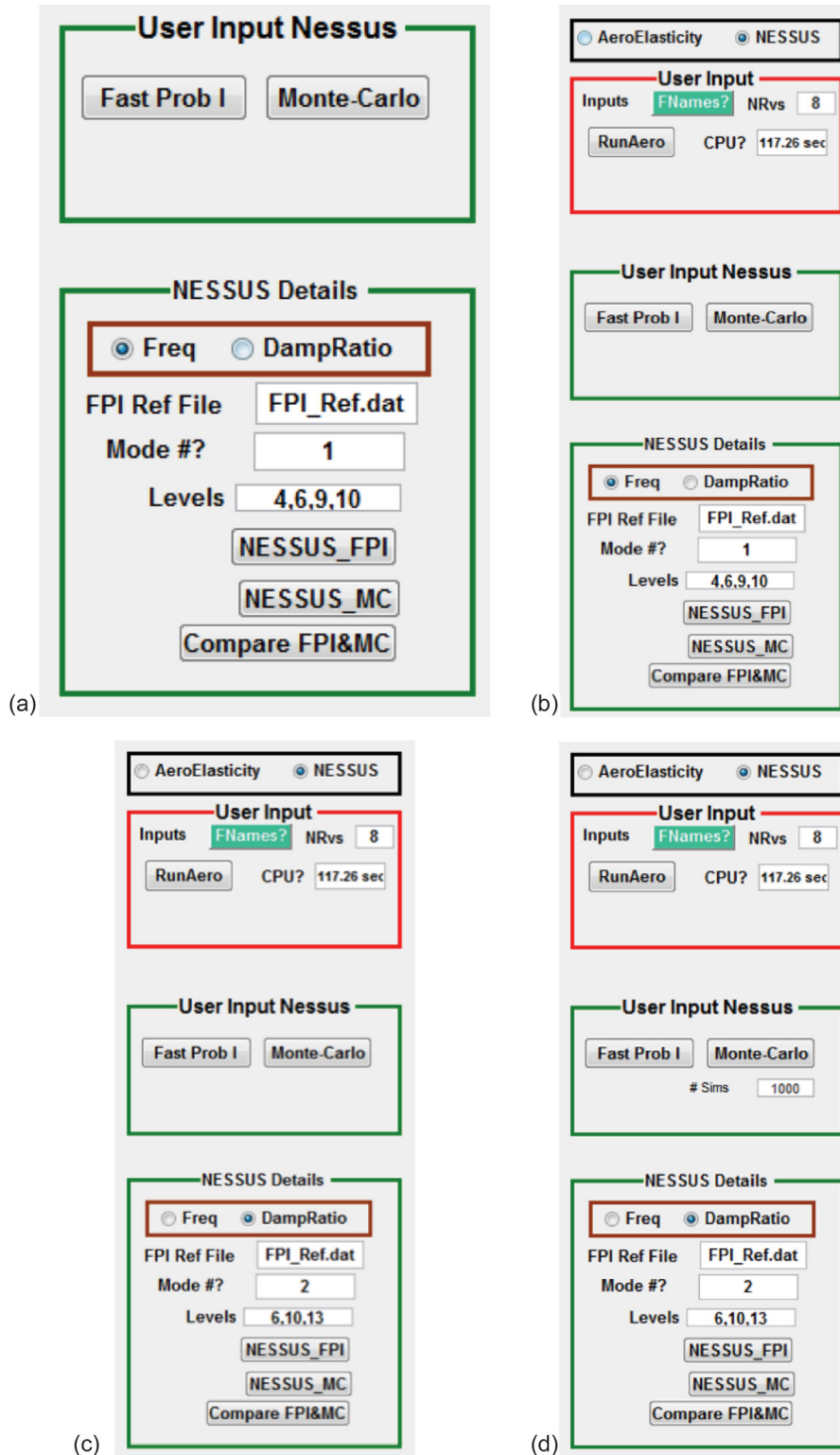


Figure 10.—User interface panels with selectable options. (a) Two additional panels that display choices for user to choose probabilistic analysis method. (b) Analysis completed after user chooses Fast Prob I (NESSUS_FPI), where central processing unit (CPU) time taken is indicated. (c) User chooses second mode DampRatio as response and probability levels 6, 10, and 13 for sensitivity plots. (d) User chooses Monte-Carlo option with 1,000 simulations.

Once the user decides on these options, pushing the button NESSUS_FPI results in a graphical display of the CDF, PDF, and the probability sensitivities of the response to random input variables as shown in Figure 11. For this case, the figure shows natural frequency response cumulative and density distribution functions and input variable sensitivities at probability levels of 0.005, 0.009, 0.4, and 0.45. The user has the option to choose similar results for a second modal frequency. Also, sensitivities can be sought for 1 to 20 levels of probability. At present, NESSUS has a constraint of 20 levels. The 20 levels chosen for this problem are as follows:

[0.00001,0.001,0.003,0.005,0.007,0.009,0.1,0.3,0.4,0.45,0.5,0.55,0.6,0.7,0.9,0.993,0.995,0.997,0.999,0.99999]

For this case, the user chose levels of 4, 6, 9, and 10 corresponding to the probability levels of 0.005, 0.009, 0.4, and 0.45, respectively. The sensitivities are ranked according to their influence on the response, the first modal frequency. It is shown that for the first modal frequency, the two factors that have the greatest influence are the revolutions per minute and the thickness.

User may also choose to select damping ratio (flutter) as the response. As an illustration, suppose that the user wants results for second mode damping ratio (flutter) response for probability levels of 6, 10, and 13. It should be noted that the analysis need not start all over again. The user just needs to change the input in the NESSUS Details panel as shown in Figure 10(c). The results for this case are shown in Figure 12. It is shown that for the second mode damping ratio that the two variables that have the greatest influence are a_∞ followed by N .

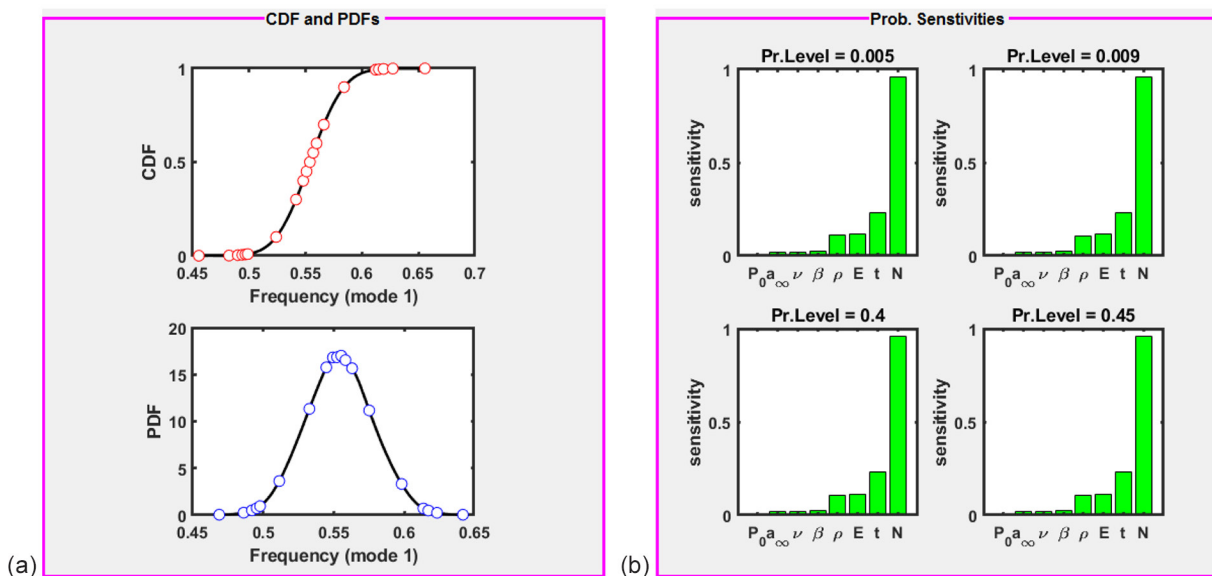


Figure 11.—Cumulative distribution function (CDF), probabilistic density function (PDF), and probability (Prob.) sensitivities of first modal frequency to eight input random variables at probability (Pr.) levels 0.005, 0.009, 0.4, and 0.45. Similar results can be obtained for second modal frequency and any combination of sensitivity requests for different probability levels. Where a_∞ is speed of sound, E is blade material Young's modulus, N is blade rotational speed, P_0 is static aerodynamic pressure, t is blade thickness parameter, β is setting angle, ν is blade material Poisson's ratio, and ρ is mass density of blade material.

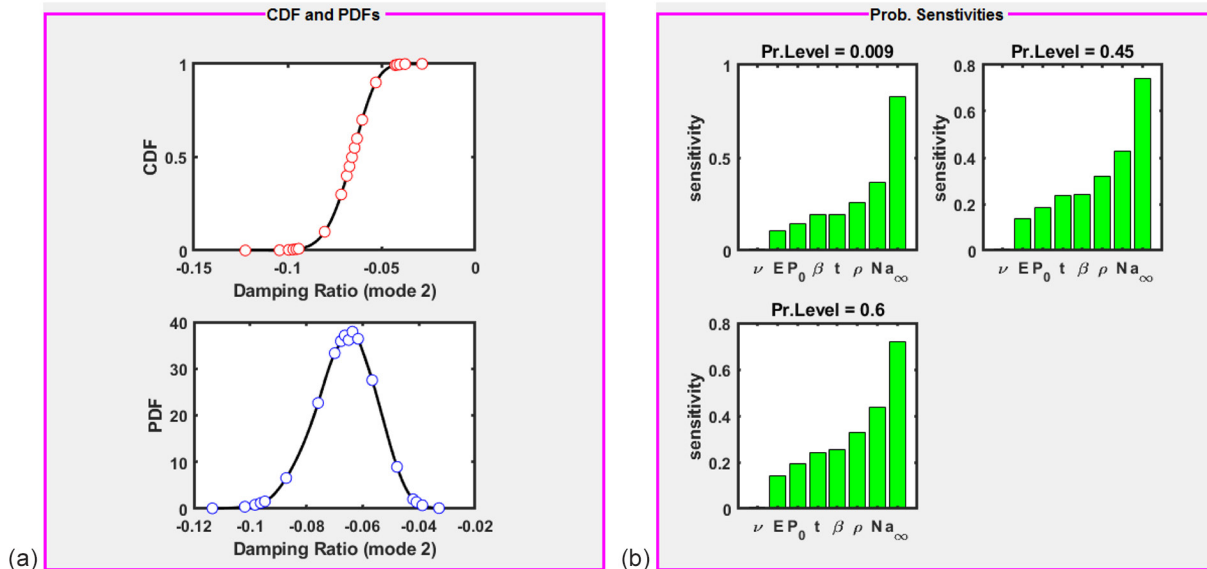


Figure 12.—Cumulative distribution function (CDF), probabilistic density function (PDF), and probability (Prob.) sensitivities of second modal damping ratio to eight input random variables at probability (Pr.) levels 0.009, 0.45, and 0.6. Similar results can be obtained for first modal damping ratio and for any combination of sensitivity requests for different probability levels. Where a_∞ is speed of sound, E is blade material Young's modulus, N is blade rotational speed, P_0 is static aerodynamic pressure, t is blade thickness parameter, β is setting angle, ν is blade material Poisson's ratio, and ρ is mass density of blade material.

5.2.2 Monte Carlo (MC) Simulations

Conventional uncertainty propagation is usually done by the MC simulation technique. Here, the same basic response analysis is done thousands of times by randomly choosing a set of input parameters, according to their probabilistic distribution. Here, there is only the provision for choosing the normal distribution. The results shown in this example are based on 1,000 simulations. The simulations can be started by choosing the radio button Monte-Carlo, and when prompted, the user specifies the number of runs, as shown in Figure 10(d). The results of MC simulations are shown as scatter plots of response to each of the eight input variables and a sensitivity plot as can be seen in Figure 13. Again, the user may choose other response quantities to obtain similar plots without having to go through the whole simulation process by simply changing the choices in the NESSUS Details panel. The program stores all the information needed so that any query can be resolved almost instantaneously.

Once both the FPI and MC analyses are complete, the user may also choose to compare both methods by pushing the button Compare FPI&MC in the NESSUS Details panel. For example, if the user chooses second mode damping ratio response, the results are shown in Figure 14. The FPI and MC predictions of the CDF, PDF, and probability sensitivity of the response to all input variables are seen to agree well with each other. This is usually not the case if the response quantities are highly nonlinear with respect to the input variables. However, FPI works satisfactorily in most cases with minimal computation effort. The 1,000 MC simulations for this case took approximately 2 h of CPU time, whereas the FPI only took 117 s of CPU time.

The last panel of significance is the Plot Controls panel. As shown in Figure 15, this panel consists of four radio buttons: Aero, NessusFPI, NessusMC, and MC_vs_FPI. It is sometimes useful to go back and forth between the various analysis results once all the analyses are complete by simply choosing the appropriate radio button. The software keeps track of all the analysis results performed so that it can quickly jump from one analysis result to another instantly.

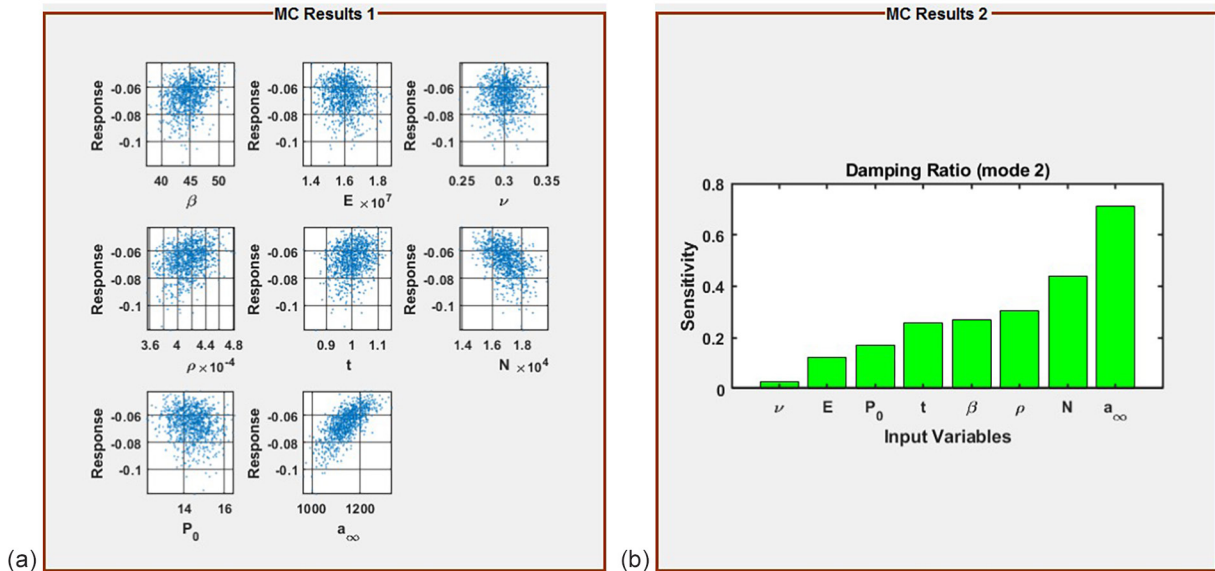


Figure 13.—Second mode damping ratio shown plotted as scatter plot versus each of eight input random variables. Also shown on right is sensitivity of damping ratio to all input variables. Where a_∞ is speed of sound, E is blade material Young's modulus, MC is Monte Carlo, N is blade rotational speed, P_0 is static aerodynamic pressure, t is blade thickness parameter, β is setting angle, ν is blade material Poisson's ratio, and ρ is mass density of blade material.

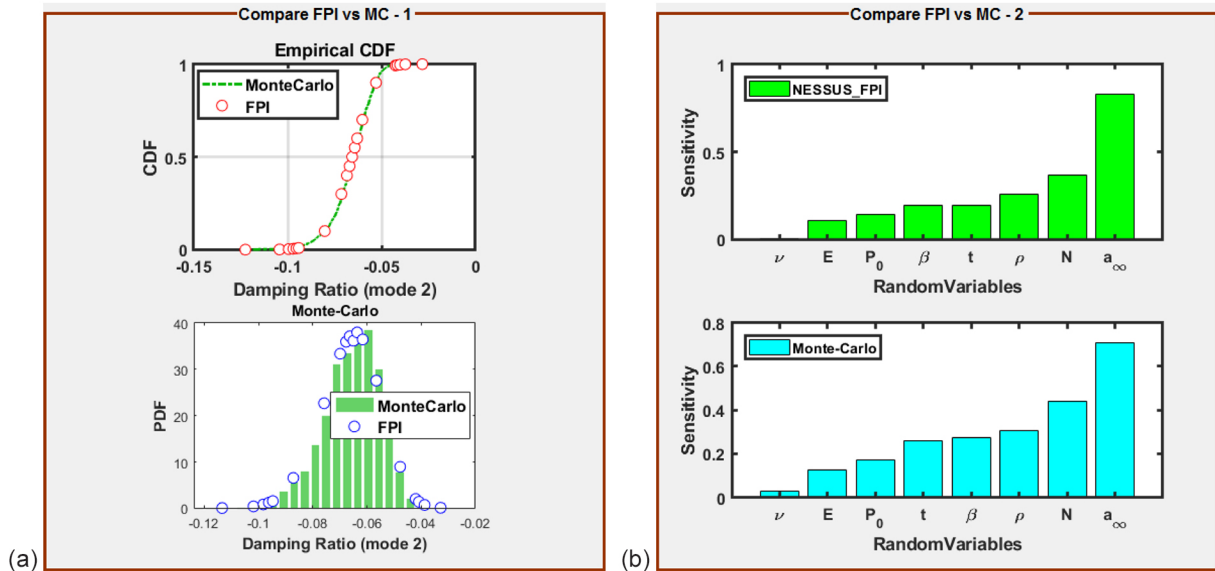


Figure 14.—A comparison of two methodologies: NESSUS_FPI and Monte-Carlo (MC) simulation techniques, where a_∞ is speed of sound, CDF is cumulative distribution function, E is blade material Young's modulus, FPI is fast probability integration, N is blade rotational speed, and NESSUS is Numerical Evaluation of Stochastic Structures Under Stress, P_0 is static aerodynamic pressure, t is blade thickness parameter, β is setting angle, ν is blade material Poisson's ratio, and ρ is mass density of blade material.

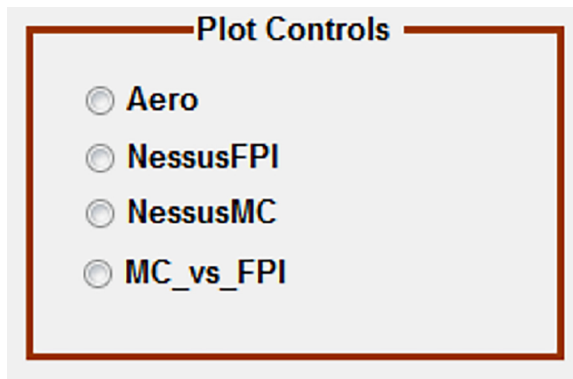


Figure 15.—Plot Controls panel showing four options for user to quickly jump from one analysis result to another.

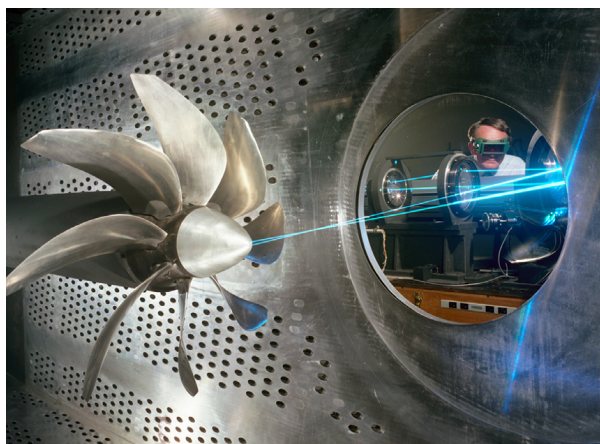


Figure 16.—SR3C–X2 propfan model in Glenn’s 8- by 6-Foot Supersonic Wind Tunnel.

5.2.2.1 Deterministic Aeroelastic Analysis Validation, Illustrative Example 1

This example pertains to a propfan, shown in Figure 16, that has been tested for flutter at various rotational speeds, free-stream Mach number, and blade setting angles (Ref. 22). The blades of the propfan are made from graphite and epoxy matrix material and are designated as SR3C–X2. There are eight blades on the rotor. The finite element model of the blade used in the analyses consists of 228 grid points and 388 plate elements (Ref. 13). The hub that retains the blades is assumed to be rigid and is not modeled. Ten strips were used in the ASTROP2 analysis.

The results of running TURBOMAT for deterministic aeroelastic response for a frequency near first mode are presented in Figure 17(a) and (b) for axial Mach numbers of 0.55 and 0.6, respectively, for a rotational speed of 6,080 rpm. The complex eigenvalues of the flutter solution give the frequency and damping ratios. Figure 17(a) and (b) show eigenvalues for eight interblade phase angles possible for the eight-blade rotor. It can be seen for $M = 0.55$ that the rotor is stable and for $M = 0.6$ that the rotor is unstable.

A plot variation of damping ratio with an axial Mach number is shown in Figure 18. It can be seen that the damping ratio becomes positive near an axial Mach number equal to 0.56. The propfan fluttered at $M = 0.58$ in the wind tunnel. The analysis shows that the ASTROP2 prediction is conservative, as expected.

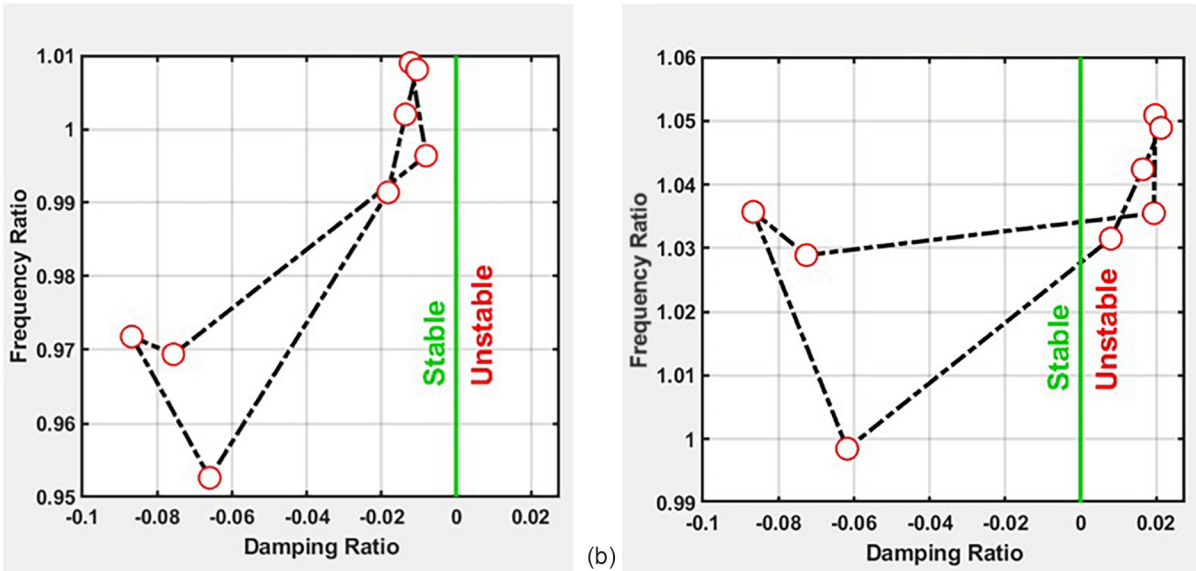


Figure 17.—Root locus plot near first mode frequency. (a) Mach number of 0.55 shows no possibility of flutter. (b) Mach number of 0.60 shows possibility of flutter.

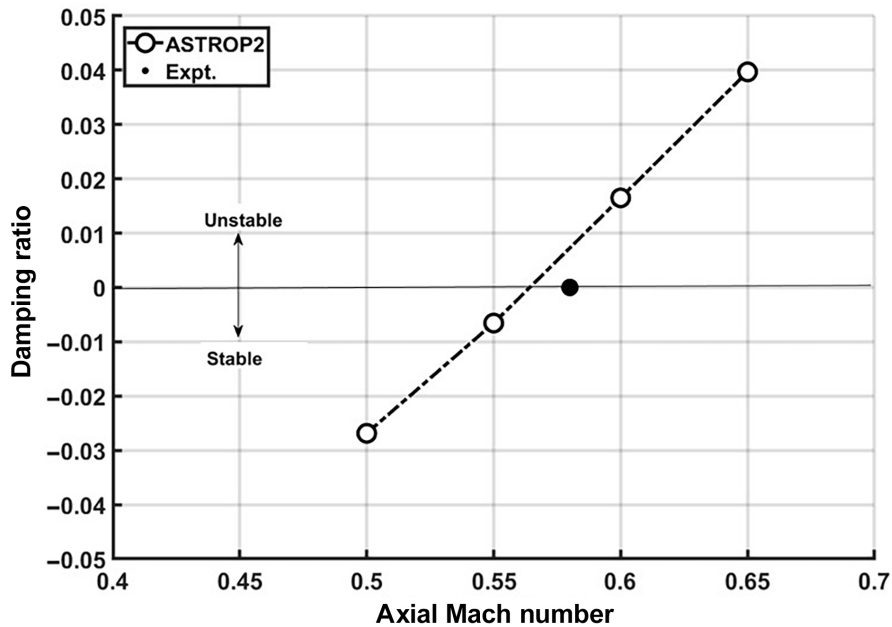


Figure 18.—Comparison of measured and calculated SR3C-X2 flutter velocity.

5.2.2.2 Probabilistic Risk Assessment, Illustrative Example 2

In order to demonstrate the usefulness of probabilistic approaches, a special example is constructed as follows. The input variables are chosen as shown in Figure 19. The standard deviations in P_0 and a_∞ are chosen as 3 and 150.1125, respectively. P_0 is the static aerodynamic pressure and a_∞ is the speed of sound. These two variables depend on altitude, the time of the day, and weather conditions, which might lead to a much higher variability than the rest of the variables. These two affect the air density, which in turn affects the mass ratio (ratio of blade mass to air mass) that directly affects the flutter stability. All these factors lead to a much higher uncertainty in these variables, and in order to reflect this, a rather large

standard deviation (close to 15 to 20 percent) was chosen. The standard deviations in thickness and revolutions per minute are 10 percent of the mean value for these variables, which affect the structural frequencies. The rest of the variables are kept the same as the example used in the report. For this case, the CDF and PDF of the response variable damping ratio for the first mode are shown in Figure 20. The damping ratio is positive in the upper tail of the distribution, indicating a chance of flutter. From the CDF, the probability for flutter is determined as 1 in 0.9996271049 or about 4 in 10,000. Thus, the reliability of the blade can be stated as about three and a half nines. Note that the deterministic flutter analysis still indicates that the blade will not flutter. It is here that the probabilistic analyses are helpful in that in addition to the deterministic answers, they enable the quantification of the probability of failure or the reliability of the blade due to flutter. In order to address this issue or to improve the reliability, it is best to look into the sensitivities of the variables and determine which top ranking variables in the order of importance can or may be controlled better so as to reduce the variability in them.

TURBOMAT Ver. 3.6
TurboMachinery Aeroelastic Analysis Tool

	RowName	Var1	Var2	Var3	Var4	Var5	Var6	Var7	Var8
1	Random Variables	BETA	E	NU	RHO	t	N	P0	A0
2	Mean Values	44.7400	16000000	0.3000	4.1440e-04	1	16962	14.4057	1.1423e+03
3	Standard Deviatio...	2.2370	800000	0.0150	2.0720e-05	0.1000	1.6001e+03	3	150.1125
4	Amount of Pertur...	1	1	1	1	1	1	1	1
5	Prob Distributions	Normal	Normal	Normal	Normal	Normal	Normal	Normal	Normal

Figure 19.—Input variables for illustrative example.

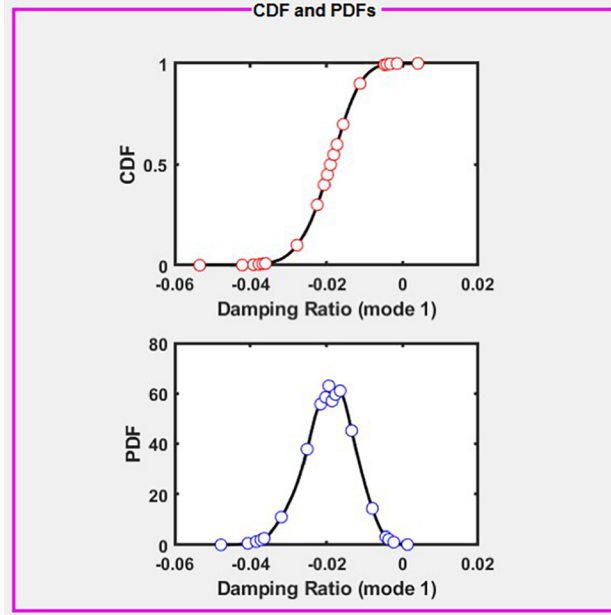


Figure 20.—Cumulative distribution function (CDF) and probabilistic density function (PDF) for mode 1 damping ratio for illustrative example. CDF shows crossing y axis into positive territory, indicating chance of flutter should adverse conditions persist.

6.0 Concluding Remarks

A probabilistic analysis for turbomachinery rotor was presented. Compared to a previous study, a three-dimensional (3D) structural model is used in the analysis. The structural analysis, aerodynamic analysis, and probabilistic analysis were connected in a seamless manner to perform the probabilistic aeroelastic analysis. A graphical user interface (GUI-) based tool, the TURBOMachinery Aeroelastic Analysis Tool (TURBOMAT), was developed to accomplish this and for ease of use. Both deterministic and probabilistic analyses were performed. As a validation of the analysis procedure, a deterministic aeroelastic assessment of the SR3C-X2 propfan for which experimental data is available is performed. The results matched well with the experimental data. As a second example, the analysis was applied to a 24-bladed rotor. Eight design variables are assumed to have probabilistic variations. The rotor was stable for the nominal values considered. Their effect of probabilistic variation on flutter damping and flutter frequency was presented. It was noted that the damping, frequency, and response calculated with the deterministic approach varied as much as 35 percent with assumed probabilistic variation. A special illustrative example is also provided to show the value added by probabilistic analyses wherein the probability of blade failure due to flutter is quantified as 4 in 10,000. Such quantified results are not possible with safety factor deterministic approaches.

It is seen that for the first modal frequency, the two factors that have the greatest influence are the revolutions per minute followed by the thickness. For the second mode damping ratio, the two factors that have the greatest influence are the speed of sound followed by the revolutions per minute.

For the cases considered, the fast probability integration (FPI) and Monte Carlo (MC) predictions of the cumulative distribution function (CDF), probability density function (PDF), and probability sensitivity of the response to all input variables are seen to agree well with each other. However, FPI works satisfactorily in most cases with the minimal computation effort. The 1,000 MC simulations for this case took approximately 2 h of central processing unit (CPU) time, whereas the FPI only took 117 s of CPU time. If higher accuracy or high nonlinearity in flutter response is expected, it is recommended to use the MC approach.

Appendix A.—Nomenclature

2D	two-dimensional
3D	three-dimensional
ASTROP2	Aeroelastic STability and Response Of Propulsion systems
CDF	cumulative distribution function
CPU	central processing unit
FEM	finite element model
FPI	fast probability integration
GUI	graphical user interface
GUIDE	graphical user interface development environment
HCF	high cycle fatigue
MC	Monte Carlo
NESSUS	Numerical Evaluation of Stochastic Structures Under Stress
PDF	probabilistic density function
RPM	revolutions per minute
TURBOMAT	TURBOMachinery Aeroelastic Analysis Tool

Symbols

$\{\mathbf{F}\}^k$	aerodynamic force vector for k^{th} blade
$\{\mathbf{f}_a\}$	motion-independent loads vector
$\{\mathbf{f}^n_a\}$	motion-dependent loads vector
$\{G\}$	assembled motion-independent load matrix
$\{u_m\}^k$	summation of normal modes
$\{\mathbf{X}\}$	vector of generalized coordinates of all blades
$\{\bar{\mathbf{X}}\}$	vector of amplitude of generalized coordinate
$\{\dot{\mathbf{X}}\}$	time derivative of vector of generalized coordinates
$[A]$	motion-dependent aerodynamic force matrix on k^{th} blade from all blades
$[K]^k$	stiffness matrix for the k_{th} blade
$[K_g]$	assembled global stiffness matrix of all blades
$[M]^k$	mass matrix for the k_{th} blade
$[M_g]$	assembled global mass matrix of all blades
ab	distance from axis of rotation to midchord
a_∞	speed of sound
\mathbf{c}	chord vector
d	distance to strip
E	Blade Material Young's modulus
e	exponential
$f_x(x)$	probability density function
g	performance function
$g(X)$	limit state function
h	plunging displacement perpendicular to chord
i	imaginary value
j	counter

M	Mach number
NB	number of blades
N	blade rotational speed in design variables
\mathbf{n}	normal vector
n	number of random variables
P	number of normal modes for used in the analysis
P_0	static aerodynamic pressure
Q	$[M_g] + [A]$
R	mode number
s	arc length measured along leading edge
\mathbf{t}	tangent vector
t	Blade thickness parameter
V	axial velocity
V_e	effective velocity
X	random variable
Z_0	given magnitude
$Z(X)$	function of number of random variable X_1 through X_n
$\{\ddot{\eta}\}^k$	generalized coordinates for k^{th} blade
$[\psi]$	assembled motion-dependent load matrix
$[\phi_m]$	modal matrix for m^{th} strip
$[\phi^k]$	modal matrix for k^{th} blade
α	pitching displacement rotation about leading edge of strip
β	setting angle
γ	$\begin{bmatrix} \omega^2 \\ \omega_0^2 \end{bmatrix}$
η	generalized displacement vector
μ	real part of eigenvalue, damping ratio
ν	Blade Material Poisson's ratio
ρ	mass density of blade material
σ_i	interblade phase angle
ν	imaginary part of eigenvalue, frequency ratio
Θ	domain of integration
ω	assumed frequency for which aerodynamic forces are calculated
Ω	rotational speed

Subscripts

f	function
M	total number of strips used in analysis
m	strip number

Superscripts

k	k^{th} blade
T	transpose

Appendix B.—astrop2.in

The input deck for Aeroelastic STability and Response Of Propulsion systems (ASTROP2), the aeroelastic analysis code, is given in this appendix. For detailed information about the program, please see References 13 and 14. As mentioned in the main text, ASTROP2 used strip theory to integrate three-dimensional (3D) structural analysis data with two-dimensional (2D) unsteady aerodynamic analysis data. Here, there are nine strips (NAEROP=9) and two modes (NMODE=2) used in the aeroelastic analysis.

astrop2.in

```

READING NASTRAN OUTPUT AND PROCESSING for Helical Fan configuration
      NAEROP      NMODE      ITEST      I6364 (READ IN MAIN)
          09          2          0          2
NASTRAN OUTPUT TYPE (RDNAS)
ANSY04 NULL08
      IPG      IPD      IPM      ISET  ICONFIG
          01          00          00          00          01
BETA75 (SETTING ANGLE AT 75% SPAN)
44.7744
      N1      N2      N3      N4
      487      567      568      648
ZBETA75
3.89900
LECOY
3.2798
TECOY
3.3867
IDREAD
1
NLE  NTE
11  11
LENODES
0000100082001630024400325004060048700568006490073000811
TENODES
0008100162002430032400405004860056700648007290081000891
METHOD
0
AEROPOINTS COORIDNATES (LOGRI):
3.4449
3.5274
3.6100
3.6925
3.7751
3.8576
3.9402
4.0228
4.1054
CAL(RDNAS1)
1.0      CAL:(=-1 NODAL VALUES,=0 ALFA/DISP, =1 ALFA/ALFA)
FLUTTER ANALYSIS OF STATOR-2 COMPRESSOR
      P0(psi)  SPS(fps)  NMODEU  NSEGS  CONFIG  RTIP  UINFL
      14.4057  1142.25  2.0    1.00   1.0    4.1054  0.0
      NONROT   NATHE   NQUASI  IREAD  ISOAFL  IAUTO  INTEG
          01      22      00      07      00      0      1
FSF(Frquency Scaling Factors, I=1,NMODEU)
      1.0  1.00000  1.00  1.0  1.0  1.0

```

```

GDAMP(Generalized DAMPing) ratios (I=1,NMODEU)
  0.0      0.000      0.0      0.0      0.0      0.0
  RPM  FRF (HZ)      MACH      BR      NBLD      BLDN
16962.40  1527.60      0.495      1.0      1.0      24.0
  SIGMA
  45.00
  SWEEP  GAP/CHD  STAGGER
  0.0      0.0      0.0
NITERF
  1
IFLUTR
  1
  0.600
  0.600
  0.600
  0.600
  0.600
  0.600
  0.600
  0.600
  0.600
  0.600
  0.600

```


Appendix C.—random.in

46.72256	BETA β setting angle
1.6075920E+07	E Blade Material Young's modulus (YMOD)
0.2848515	NU ν Blade Material Poisson's ratio (POIS)
4.2550178E-04	Rho ρ mass density of blade material (MASSD)
1.0	t Blade thickness Parameter (THICKD)
17880.41	N Blade Rotational Speed(RPM)
15.23086	P0 static aerodynamic pressure
1119.496	a_∞ A0 speed of sound

Appendix D.—struct.dat

A condensed version of the finite element model (FEM) input file to the Numerical Evaluation of Stochastic Structures Under Stress (NESSUS) program is provided in this appendix to indicate the input format that NESSUS accepts for normal modes structural analysis.

```

*FEM
C rotating cantilever blade, 16,962 rpm
C rotating speed MUST be input in radians per second
C 16,961 rpm = 1776.2564864 rad/sec
C
C
C ++++++ PARAMETER DATA ++++++
C
*NODES      891
*ELEMENTS   800
      75
*PRINT
*POST
*BOUN      486
*DIST
*STIFF
*MODAL      2      0      0
*END
*ITER
100      0.7      0.7      0.7
C
C ++++++ MODEL DATA ++++++
C
C the GRID coordinates are for setting angle = 44.77400
*COO
      1      -0.3694      0.8855      3.2798      0.008839
      2      -0.3660      0.8825      3.2806      0.008000
      3      -0.3622      0.8793      3.2815      0.008000
      4      -0.3582      0.8758      3.2824      0.008000
      5      -0.3540      0.8722      3.2834      0.008000
      6      -0.3497      0.8686      3.2843      0.008000
      7      -0.3454      0.8649      3.2853      0.008000
      8      -0.3412      0.8613      3.2862      0.008000
      9      -0.3370      0.8577      3.2872      0.008000
     10      -0.3326      0.8538      3.2881      0.008000
     11      -0.3275      0.8495      3.2893      0.008000
     12      -0.3220      0.8447      3.2905      0.008000
     13      -0.3165      0.8400      3.2917      0.008000
     14      -0.3111      0.8353      3.2928      0.008000
     15      -0.3061      0.8310      3.2939      0.008000
     16      -0.3011      0.8267      3.2950      0.008000
     17      -0.2947      0.8212      3.2964      0.008000
     18      -0.2854      0.8131      3.2983      0.008000
     19      -0.2732      0.8026      3.3009      0.008000
     20      -0.2600      0.7913      3.3036      0.008000
*****
*****
*****
     870      0.2071      0.4745      4.2182      0.008000
     871      0.2179      0.4626      4.2195      0.008000

```

872	0.2290	0.4504	4.2208	0.008000
873	0.2409	0.4372	4.2222	0.008000
874	0.2536	0.4231	4.2236	0.008000
875	0.2652	0.4102	4.2248	0.008000
876	0.2738	0.4007	4.2258	0.008000
877	0.2796	0.3942	4.2264	0.008000
878	0.2844	0.3890	4.2269	0.008000
879	0.2893	0.3836	4.2273	0.008000
880	0.2945	0.3778	4.2279	0.008000
881	0.2998	0.3718	4.2284	0.008000
882	0.3051	0.3660	4.2289	0.008000
883	0.3098	0.3607	4.2293	0.008000
884	0.3140	0.3561	4.2297	0.008000
885	0.3181	0.3516	4.2301	0.008000
886	0.3222	0.3469	4.2305	0.008000
887	0.3264	0.3423	4.2308	0.008000
888	0.3308	0.3377	4.2311	0.008000
889	0.3353	0.3331	4.2313	0.008000
890	0.3397	0.3286	4.2315	0.008000
891	0.3441	0.3241	4.2317	0.008000

*ELEMENTS

75

1	1	82	83	2
2	82	163	164	83
3	163	244	245	164
4	244	325	326	245
5	325	406	407	326
6	406	487	488	407
7	487	568	569	488
8	568	649	650	569
9	649	730	731	650
10	730	811	812	731
11	2	83	84	3
12	83	164	165	84
13	164	245	246	165
14	245	326	327	246
15	326	407	408	327
16	407	488	489	408
17	488	569	570	489
18	569	650	651	570
19	650	731	732	651
20	731	812	813	732

789	727	808	809	728
790	808	889	890	809
791	80	161	162	81
792	161	242	243	162
793	242	323	324	243
794	323	404	405	324
795	404	485	486	405
796	485	566	567	486
797	566	647	648	567
798	647	728	729	648
799	728	809	810	729
800	809	890	891	810

*PRO

1	1	0.8839E-02	0.1600E+08	0.3000E+00	0.5600E-05	0.4144E-03
2	2	0.8000E-02	0.1600E+08	0.3000E+00	0.5600E-05	0.4144E-03
3	3	0.8000E-02	0.1600E+08	0.3000E+00	0.5600E-05	0.4144E-03
4	4	0.8000E-02	0.1600E+08	0.3000E+00	0.5600E-05	0.4144E-03
5	5	0.8000E-02	0.1600E+08	0.3000E+00	0.5600E-05	0.4144E-03
6	6	0.8000E-02	0.1600E+08	0.3000E+00	0.5600E-05	0.4144E-03
7	7	0.8000E-02	0.1600E+08	0.3000E+00	0.5600E-05	0.4144E-03
8	8	0.8000E-02	0.1600E+08	0.3000E+00	0.5600E-05	0.4144E-03
9	9	0.8000E-02	0.1600E+08	0.3000E+00	0.5600E-05	0.4144E-03
10	10	0.8000E-02	0.1600E+08	0.3000E+00	0.5600E-05	0.4144E-03
11	11	0.8000E-02	0.1600E+08	0.3000E+00	0.5600E-05	0.4144E-03
12	12	0.8000E-02	0.1600E+08	0.3000E+00	0.5600E-05	0.4144E-03
13	13	0.8000E-02	0.1600E+08	0.3000E+00	0.5600E-05	0.4144E-03
14	14	0.8000E-02	0.1600E+08	0.3000E+00	0.5600E-05	0.4144E-03
15	15	0.8000E-02	0.1600E+08	0.3000E+00	0.5600E-05	0.4144E-03
16	16	0.8000E-02	0.1600E+08	0.3000E+00	0.5600E-05	0.4144E-03
17	17	0.8000E-02	0.1600E+08	0.3000E+00	0.5600E-05	0.4144E-03
18	18	0.8000E-02	0.1600E+08	0.3000E+00	0.5600E-05	0.4144E-03
19	19	0.8000E-02	0.1600E+08	0.3000E+00	0.5600E-05	0.4144E-03
20	20	0.8000E-02	0.1600E+08	0.3000E+00	0.5600E-05	0.4144E-03

870	870	0.8000E-02	0.1600E+08	0.3000E+00	0.5600E-05	0.4144E-03
871	871	0.8000E-02	0.1600E+08	0.3000E+00	0.5600E-05	0.4144E-03
872	872	0.8000E-02	0.1600E+08	0.3000E+00	0.5600E-05	0.4144E-03
873	873	0.8000E-02	0.1600E+08	0.3000E+00	0.5600E-05	0.4144E-03
874	874	0.8000E-02	0.1600E+08	0.3000E+00	0.5600E-05	0.4144E-03
875	875	0.8000E-02	0.1600E+08	0.3000E+00	0.5600E-05	0.4144E-03
876	876	0.8000E-02	0.1600E+08	0.3000E+00	0.5600E-05	0.4144E-03
877	877	0.8000E-02	0.1600E+08	0.3000E+00	0.5600E-05	0.4144E-03
878	878	0.8000E-02	0.1600E+08	0.3000E+00	0.5600E-05	0.4144E-03
879	879	0.8000E-02	0.1600E+08	0.3000E+00	0.5600E-05	0.4144E-03
880	880	0.8000E-02	0.1600E+08	0.3000E+00	0.5600E-05	0.4144E-03
881	881	0.8000E-02	0.1600E+08	0.3000E+00	0.5600E-05	0.4144E-03
882	882	0.8000E-02	0.1600E+08	0.3000E+00	0.5600E-05	0.4144E-03
883	883	0.8000E-02	0.1600E+08	0.3000E+00	0.5600E-05	0.4144E-03
884	884	0.8000E-02	0.1600E+08	0.3000E+00	0.5600E-05	0.4144E-03
885	885	0.8000E-02	0.1600E+08	0.3000E+00	0.5600E-05	0.4144E-03
886	886	0.8000E-02	0.1600E+08	0.3000E+00	0.5600E-05	0.4144E-03
887	887	0.8000E-02	0.1600E+08	0.3000E+00	0.5600E-05	0.4144E-03
888	888	0.8000E-02	0.1600E+08	0.3000E+00	0.5600E-05	0.4144E-03
889	889	0.8000E-02	0.1600E+08	0.3000E+00	0.5600E-05	0.4144E-03
890	890	0.8000E-02	0.1600E+08	0.3000E+00	0.5600E-05	0.4144E-03
891	891	0.8000E-02	0.1600E+08	0.3000E+00	0.5600E-05	0.4144E-03

*BOUNDARY

1	1	0.0000
1	2	0.0000
1	3	0.0000
1	4	0.0000
1	5	0.0000
1	6	0.0000
2	1	0.0000
2	2	0.0000
2	3	0.0000
2	4	0.0000
2	5	0.0000

```

2      6      0.0000
3      1      0.0000
3      2      0.0000
3      3      0.0000
3      4      0.0000
3      5      0.0000
3      6      0.0000
4      1      0.0000
4      2      0.0000
4      3      0.0000
4      4      0.0000
4      5      0.0000
4      6      0.0000
*****
*****
80     1      0.0000
80     2      0.0000
80     3      0.0000
80     4      0.0000
80     5      0.0000
80     6      0.0000
81     1      0.0000
81     2      0.0000
81     3      0.0000
81     4      0.0000
81     5      0.0000
81     6      0.0000
*DIST  75
      1    800   11    0.0000    0.0000  532.8765
*BODY      2
0.0000    0.0000    0.0000
1.0000    0.0000    0.0000
*PRINTOPTIONS
TOTALDISPLACEMENTS  NODE
*END
*END

```

References

1. Pettit, Chris L.: Uncertainty Quantification in Aeroelasticity: Recent Results and Research Challenges. *J. Aircr.*, vol. 41, no. 5, 2004.
2. Styuart, Andrey V., et al.: Probabilistic Modeling of the Aeroelastic Life Cycle for Risk Evaluation of Composite Structures. AIAA 2008–2300, 2008.
3. Pitt, Dale M., et al.: Probabilistic Aeroelastic Analysis and Its Implications on Flutter Margin Requirements. AIAA 2008–2198, 2008.
4. Verhoosel, Clemens V., et al.: Uncertainty and Reliability Analysis of Fluid-Structure Stability Boundaries. *AIAA J.*, vol. 4, no. 1, 2009, pp. 91–104.
5. Marques, S., et al.: Transonic Aeroelastic Stability Predictions Under the Influence of Structural Variability. *J. Aircr.*, vol. 47, no. 4, 2010, pp. 1229–1239.
6. Ghommem, Mehdi; Hajj, Muhammad R.; and Nayfeh, Ali H.: Effects of Parameter Uncertainties on the Response of an Aeroelastic System. AIAA 2010–2765, 2010.
7. Borglund, Dan; and Ringertz, Ulf: Solution of the Flutter Eigenvalue Problem With Mixed Structural/Aerodynamic Uncertainty. *J. Aircr.*, vol. 48, no. 1, 2011, pp. 343–348.
8. Riley, Matthew E.; Grandhi, Ramana V.; and Kolonay, Raymond: Quantification of Modeling Uncertainty in Aeroelastic Analyses. *J. Aircraft*, vol. 48, no. 3, 2011, pp. 866–873.
9. Danowsky, Brian P., et al.: Evaluation of Aeroelastic Uncertainty Analysis Methods. *J. Aircr.*, vol. 47, no. 4, 2010, pp. 1266–1273.
10. Wu, Sang V.; and Livne, Eli: Alternate Aerodynamic Uncertainty Modeling Approaches for Flutter Reliability Analysis. *AIAA J.*, vol. 55, no. 8, 2017, pp. 2808–2823.
11. Wu, Y.-T.: Computational Methods for Efficient Structural Reliability and Reliability Sensitivity Analysis. *AIAA J.*, vol. 32, no. 8, 1994, pp. 1717–1723.
12. Reddy, T.S.R.; Mital, S.K.; and Stefko, G.L.: Probabilistic Aeroelastic Analysis of Turbomachinery Components. NASA/TM—2004-213063, 2004. <http://ntrs.nasa.gov>
13. Narayanan, G.V.; and Kaza, K.R.V.: ASTROP2 Users Manual: A Program for Aeroelastic Stability Analysis for Propfans. NASA TM–4304, 1991. <http://ntrs.nasa.gov>
14. Reddy, T.S.R.; and Lucero, John M.: ASTROP2 Users Manual: A Program for Aeroelastic Stability Analysis for Propfans, Version 2. NASA TM–107195, 1996. <http://ntrs.nasa.gov>
15. Wu, Y.-T.: Demonstration of a New, Fast Probability Integration Method for Reliability Analysis, *J. Eng. Ind.*, vol. 109, no. 1, 1987, pp. 24–28.
16. NESSUS/FPI User’s Manual. Version 6.2, Southwest Research Institute for NASA Lewis Research Center, 1995.
17. MATLAB and Statistics Toolbox Release. The MathWorks, Inc., Natick, MA, 2016.
18. Smith, S.N.: Discrete Frequency Sound Generation in Axial Flow Turbomachines. British Aeronautical Research Council R&M No. 3709, 1973.
19. Adamczyk, J.J.; and Goldstein, M.E.: Unsteady Flow in a Supersonic Cascade With Subsonic Leading-Edge Locus. *AIAA J.*, vol. 16, no. 12, 1978, pp. 1248–1254.
20. Reddy, T.S.R.; Srivastava, R.; and Mehmed, O.: ASTROP2-LE: A Mistuned Aeroelastic Analysis System Based on a Two Dimensional Linearized Euler Solver. NASA/TM—2002-211499, 2002. <http://ntrs.nasa.gov>
21. Kaza, K.R.V., et al.: Analytical Flutter Investigation of a Composite Propfan Model. *J. Aircr.*, vol. 26, no. 8, 1989, pp. 772–780.
22. Mehmed, O.; and Kaza, K.R.V.: Experimental Classical Flutter Results of a Composite Advanced Turboprop Model. NASA TM–88792, 1986. <http://ntrs.nasa.gov>

